REPORT No. 184
GEOLOGICAL SURVEY OF JAPAN

ON THE PROPAGATION OF TRANSIENT ELASTIC WAVES

By

Shozaburo NAGUMO

REPORT No. 184

GEOLOGICAL SURVEY OF JAPAN

Katsu KANEKO, Director

On the Propagation of Transient Elastic Waves

By

Shozaburo NAGUMO

CONTENTS

On the Propagation of Transient Elastic Waves

By

Shozaburo NAGUMO

Abstract

The propagation of transient elastic waves in two dimensions is investigated by the method of dual integral transformation. Laplace transformation is applied to the time coordinate and Fourier transformation is applied to one space coordinate. Simple mathematical expression of solving the problem is presented.

In chapter I and II, the re-written forms of the surface force problem and the buried line source problem in solid are presented showing the way of application of the dual integral transformation. In chapter III, the problem of reflection and refraction of an acoustic pressure pulse at a liquid-liquid interface is taken so as to clear up the basic picture of reflection and refraction of a pulse which has a curved wave front. In chapter IV, diffraction of an acoustic pressure pulse by a finite fixed plane placed in liquid is investigated. Application of convolution formula to the inverse transformation leads the exact solution to a form of integral of elementary functions. An interpretation for the mechanism of diffraction phenomenon is presented.

General Introduction

The rigorous treatment of transient elastic wave propagation was pioneered by Cagniard[3] by the method of implicit Laplace transformation. And his method, Cagniard's method, has been rewritten in the form of explicit Laplace transformation by Dix[5], and has been successfully applied to the generation and propagation of transient elastic wave by Dix[6], Spencer[23] and Garvin[8] with results of better picture on the mechanism of Rayleigh wave generation on a semi-infinite elastic medium and that of reflection at a liquid-liquid interface.

This paper reports a further application of method of integral transformation to the theory of propagation of transient elastic waves in two dimensions. Namely, in addition to Laplace transformation applied to the time coordinate, Fourier transformation is applied to one space coordinate. Both wave equations and boundary conditions are Laplace-Fourier transformed, and formal solutions are obtained in the transformed space. Then the inverse transformation of the formal solutions are evaluated. By so doing, mathematical expression of solving the problem is reduced to a simple form, and Cagniard's technique, which beats the integral solution to the form of Laplace transformation integral, is logically introduced by the translation property of Laplace transformation. Besides that, physical and mathematical rigorousness are given to the conversion of parameters and to the integration path by the Laplace transformation formula of δ-function. The principle and examples of application of integral transformation to the boundary value problem of partial differential equation in the various field of physics are well described by Sneddon[21][22].

In chapter I and II, the rewritten form of the surface force problem and the buried line source problem in solid are presented showing the way of application of the integral transformation. As a consequence of Fourier transformation

applied to a space coordinate, a solution for spacial transient surface force is obtained. In chapter III, the problem of reflection and refraction of an acoustic pressure pulse at a liquid-liquid interface is taken so as to clear up the basic picture of reflection and refraction of a pulse which has a curved wave front. In chapter IV, diffraction of an acoustic pressure pulse by a finite fixed plane placed in liquid is investigated. Application of convolution formula to the inverse transformation leads the exact solution to a form of integral of elementary functions. An interpretation for the mechanism of diffraction phenomenon is presented.

I. Surface Force Problem

I. 1 Introduction

Propagation of a transient elastic wave generated by a suddenly applied surface force has been studied by Lamb[17], Hirono[9], Kasahara[15], Takeuchi and Kobayashi[25], and Honda, Nakamura and Takagi[15]. In this chapter, the mathematical expression of the way of solving this surface force problem is rewritten in a simple form showing the method of integral transformation which will be used hereafter in this paper. And the exact solution of displacement given at everywhere in the medium is obtained for both concentrated and spacial surface forces.

I. 2 Wave equation and stress

The equations of motion in an elastic medium are

$$\begin{cases} (\lambda+\mu)\dfrac{\partial \Delta}{\partial x} + \mu \nabla^2 u = \rho\dfrac{\partial^2 u}{\partial t^2} \\[2mm] (\lambda+\mu)\dfrac{\partial \Delta}{\partial x} + \mu \nabla^2 w = \rho\dfrac{\partial^2 w}{\partial t^2} \end{cases} \qquad (1.1)$$

where

$$\begin{cases} u,\ w: \quad \text{displacement in } x,\ y \text{ direction} \\[2mm] \Delta = \dfrac{\partial u}{\partial x} + \dfrac{\partial w}{\partial z} \\[2mm] \rho,\ \lambda,\ \mu: \quad \text{density, Lamé's constant, rigidity.} \end{cases}$$

Introducing displacement potentials ϕ and ψ, by the relations

$$\begin{cases} u = \dfrac{\partial \phi}{\partial x} + \dfrac{\partial \psi}{\partial z} \\[2mm] w = \dfrac{\partial \phi}{\partial z} - \dfrac{\partial \psi}{\partial x} \end{cases} \qquad (1.2)$$

the equations of motion are reduced to wave equations

$$\begin{cases} \nabla^2 \phi = \dfrac{1}{V_p{}^2}\ \dfrac{\partial^2 \phi}{\partial t^2} \\[2mm] \nabla^2 \psi = \dfrac{1}{V_s{}^2}\ \dfrac{\partial^2 \psi}{\partial t^2} \end{cases} \qquad (1.3)$$

where

$$V_p{}^2 = (\lambda + 2\mu)/\rho \quad \text{and} \quad V_s{}^2 = \mu/\rho.$$

Normal and tangential stress components are, when represented by displacement,

$$
\begin{cases}
P_{zz} = \lambda \left(\dfrac{\partial u}{\partial x} + \dfrac{\partial w}{\partial z} \right) + 2\mu \, \dfrac{\partial w}{\partial z} \\[2mm]
P_{xz} = \mu \left(\dfrac{\partial u}{\partial z} + \dfrac{\partial w}{\partial x} \right) \quad ,
\end{cases}
\tag{1.4}
$$

and, when represented by displacement potentials,

$$
\begin{cases}
P_{zz} = \lambda \phi_{xx} + (\lambda + 2\mu)\, \phi_{zz} - 2\mu\psi_{xz} \\
P_{xz} = \mu \, (2\phi_{xz} + \psi_{zz} - \psi_{xx}) \quad .
\end{cases}
\tag{1.5}
$$

I. 3 Laplace transform of wave equation and stress

Now we apply Laplace transformation with respect to t to the wave equations (1.3) and stress (1.4). Let $\Phi(x, z, p)$ and $\Psi(x, z, p)$ be Laplace transform of $\phi(x, z, t)$ and $\psi(x, z, t)$. By the definition of Laplace transform, they are

$$
\begin{cases}
\Phi(x, z, p) = \displaystyle\int_0^\infty \phi(x, z, t)\, e^{-pt}\, dt \\[2mm]
\Psi(x, z, p) = \displaystyle\int_0^\infty \psi(x, z, t)\, e^{-pt}\, dt \quad .
\end{cases}
\tag{1.6}
$$

Then, for Laplace transformed wave equation and stress, we have

$$
\begin{cases}
(\nabla^2 - h^2)\, \Phi = 0 \\
(\nabla^2 - k^2)\, \Psi = 0 \quad ,
\end{cases}
\tag{1.7}
$$

where

$$
h^2 = p^2/V_p^2, \quad k^2 = p^2/V_s^2
\tag{1.8}
$$

and

$$
\begin{cases}
P_{zz} = \lambda \Phi_{xx} + (\lambda + 2\mu)\, \Phi_{zz} - 2\mu\Psi_{xz} \\
P_{xz} = \mu \, (2\Phi_{xz} + \Psi_{zz} - \Psi_{xx}) \quad .
\end{cases}
\tag{1.9}
$$

I. 4 Fourier transform of wave equation and stress

Let us apply Fourier transformation with respect to x to the Laplace transformed wave equation (1.7) and stress (1.9). Let $\bar{\phi}(\xi, z, p)$ and $\bar{\psi}(\xi, z, p)$ be Fourier transform of Φ and Ψ. By the definition of Fourier transform, they are

$$
\begin{cases}
\bar{\phi}(\xi, z, p) = \dfrac{1}{\sqrt{2\pi}} \displaystyle\int_{-\infty}^\infty \Phi(x, z, p)\, e^{i\xi x}\, dx \\[2mm]
\bar{\psi}(\xi, z, p) = \dfrac{1}{\sqrt{2\pi}} \displaystyle\int_{-\infty}^\infty \Psi(x, z, p)\, e^{i\xi x}\, dx \quad .
\end{cases}
\tag{1.10}
$$

Then, for Laplace-Fourier transformed wave equation and stress, we have

$$
\begin{cases}
\dfrac{d^2\bar{\phi}}{dz^2} - (\xi^2 + h^2)\, \bar{\phi} = 0 \\[2mm]
\dfrac{d^2\bar{\psi}}{dz^2} - (\xi^2 + k^2)\, \bar{\psi} = 0
\end{cases}
\tag{1.11}
$$

and

$$\begin{cases} \bar{P}_{zz} = -\,\lambda\xi\bar{\phi} + (\lambda + 2\mu)\,\bar{\phi}_{zz} + 2i\mu\xi\bar{\psi}_z & {}^* \\ \bar{P}_{xz} = \mu\,(-\,2i\xi\bar{\phi}_z + \bar{\psi}_{zz} + \xi^2\bar{\psi}) & . \end{cases} \tag{1.12}$$

I. 5 Laplace-Fourier transform of displacement and velocity

For the later use, let us show Laplace-Fourier transform of displacement and velocity. Laplace transforms of displacement components U, W become, from the relation (1.2),

$$\begin{cases} U\,(x,\,z,\,p) = \Phi_x + \Psi_z \\ W\,(x,\,z,\,p) = \Phi_z - \Psi_x \end{cases} \tag{1.13}$$

and Fourier transforms of them become

$$\begin{cases} \bar{u}\,(\xi,\,z,\,p) = -\,i\xi\bar{\phi} + \bar{\psi}_z \\ \bar{w}\,(\xi,\,z,\,p) = \bar{\phi}_z + i\xi\bar{\psi} \end{cases} . \tag{1.14}$$

Likewise, Laplace transforms of velocity components are

$$\begin{cases} \dot{U}\,(x,\,z,\,p) = pU \\ \dot{W}\,(x,\,z,\,p) = pW \end{cases} \tag{1.15}$$

because they are the time derivative[**] of displacement, and Fourier transforms of them are

$$\begin{cases} \dot{\bar{u}}\,(\xi,\,z,\,p) = p\bar{u} \\ \dot{\bar{w}}\,(\xi,\,z,\,p) = p\bar{w} \end{cases} . \tag{1.16}$$

In a similar way, Laplace-Fourier transforms of acceleration components become

$$\begin{cases} \ddot{\bar{u}} = p^2\bar{u} \\ \ddot{\bar{w}} = p^2\bar{w} \end{cases} . \tag{1.17}$$

I. 6 Formal solutions of the surface force problem

Let us treat the surface force problem; the propagation of transient elastic wave generated by the vertical force applied at the surface of a semi-infinite elastic medium. Referring to Fig. 1, we take x-y axes on the surface and z-axis vertically downward into the medium.
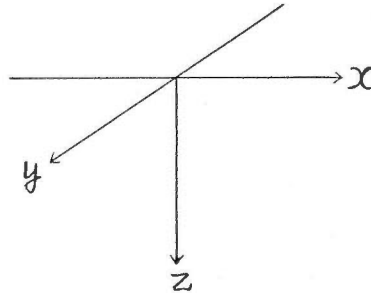

Fig. 1

When the vertical surface force is denoted by $f(x, t)$, its Laplace transform is given by

$$F(x, p) = \int_0^\infty f(x, t) \ e^{-pt} \ dt \tag{1.18}$$

and its Fourier-Laplace transform is given by

$$\bar{f}(\xi, p) = \frac{1}{\sqrt{2\pi}} \int_{-\infty}^\infty F(x, p) \ e^{i\xi x} \ dx \quad . \tag{1.19}$$

Boundary conditions to be satisfied at the surface $z = 0$, in the transformed space are, from (1.12) and (1.19),

$$\begin{cases} -\lambda\xi^2\bar{\phi} + (\lambda + 2\mu)\,\bar{\phi}_{zz} + 2i\mu\xi\bar{\psi}_z = \bar{f}(\xi, p) \\ -2i\xi\bar{\phi}_z + \bar{\psi}_{zz} + \xi^2\bar{\psi} = 0 \quad . \end{cases} \tag{1.20}$$

The general solutions in the transformed space are obtained from (1.11) and in this case, we have

$$\begin{cases} \bar{\phi}(\xi, z, p) = A(\xi, p) \ e^{-\sqrt{\xi^2+h^2}\,z} \\ \bar{\psi}(\xi, z, p) = B(\xi, p) \ e^{-\sqrt{\xi^2+k^2}\,z} \quad . \end{cases} \tag{1.21}$$

A and B are determined by putting (1.21) into (1.20). Thus, we get

$$A = \frac{1}{F(\xi, p)} \ \bar{f}(\xi, p) \ (2\xi^2 + k^2) \tag{1.22}$$

$$B = \frac{1}{F(\xi, p)} \ \bar{f}(\xi, p) \ (2i\xi \sqrt{\xi^2 + k^2}) \tag{1.23}$$

$$F(\xi, p) = \mu \ \{(2\xi^2 + k^2)^2 - 4\xi^2 \sqrt{\xi^2 + h^2} \sqrt{\xi^2 + k^2}\}. \tag{1.24}$$

Therefore, solutions of displacement potential in Laplace-Fourier transformed space are

$$\begin{cases} \bar{\phi}(\xi, z, p) = \frac{1}{F(\xi, p)} \ \bar{f}(\xi, p) \ (2\xi^2 + k^2) \ e^{-\sqrt{\xi^2+h^2}\,z} \\ \bar{\psi}(\xi, z, p) = \frac{1}{F(\xi, p)} \ \bar{f}(\xi, p) \ (2i\xi \sqrt{\xi^2 + h^2}) \ e^{-\sqrt{\xi^2+k^2}\,z} \ . \end{cases} \tag{1.25}$$

Displacement solutions are obtained from (1.25) and (1.14)

$$\begin{cases} \bar{u} = \dfrac{1}{F(\xi, p)} \ \bar{f}(\xi, p) \ (2\xi^2 + k^2) \ (-i\xi) \ e^{-\sqrt{\xi^2+h^2}\,z} \\[2mm] \quad + \dfrac{1}{F(\xi, p)} \ \bar{f}(\xi, p) \ (2i\xi \sqrt{\xi^2 + h^2}) \ (-\sqrt{\xi^2 + k^2}) \ e^{-\sqrt{\xi^2+k^2}\,z} \\[2mm] \bar{w} = \dfrac{1}{F(\xi, p)} \ \bar{f}(\xi, p) \ (2\xi^2 + k^2) \ (-\sqrt{\xi^2 + h^2}) \ e^{-\sqrt{\xi^2+h^2}\,z} \\[2mm] \quad + \dfrac{1}{F(\xi, p)} \ \bar{f}(\xi, p) \ (2i\xi \sqrt{\xi^2 + h^2}) \ (i\xi) \ e^{-\sqrt{\xi^2+k^2}\,z} \quad . \end{cases} \tag{1.26}$$

Velocity and acceleration solutions will be likewise obtained from (1.16), (1.17) and (1.25).

Formal solutions of displacement potential in the original space are directly written in the form of inverse transformation ;

$$\begin{cases} \phi\,(x,\,z,\,t) = L^{-1}\cdot F^{-1}\,\bar{\phi}\,(\xi,\,z,\,p) \\[4pt] \qquad \equiv \dfrac{1}{2\pi j}\int_{c-j\infty}^{c+j\infty}e^{pt}\Big[\dfrac{1}{\sqrt{2\pi}}\int_{-\infty}^{\infty}\phi\,(\xi,\,z,\,p)\ e^{-i\xi x}d\xi\Big]\,dp \\[10pt] \psi\,(x,\,z,\,t) = L^{-1}\cdot F^{-1}\,\bar{\phi}\,(\xi,\,z,\,p) \\[4pt] \qquad \equiv \dfrac{1}{2\pi j}\int_{c-j\infty}^{c+j\infty}e^{pt}\Big[\dfrac{1}{\sqrt{2\pi}}\int_{-\infty}^{\infty}\bar{\phi}\,(\xi,\,z,\,p)\ e^{-i\xi x}d\xi\Big]\,dp. \end{cases} \tag{1.27}$$

Likewise, formal solutions of displacement and velocity in the original space are written by

$$\begin{cases} u\,(x,\,z,\,t) = L^{-1}\cdot F^{-1}\,\bar{u}\,(\xi,\,z,\,p) \\[4pt] w\,(x,\,z,\,t) = L^{-1}\cdot F^{-1}\,\bar{w}\,(\xi,\,z,\,p) \end{cases} \tag{1.28}$$

and

$$\begin{cases} \dot{u}\,(x,\,z,\,t) = L^{-1}\cdot F^{-1}\,[\,p\bar{u}\,(\xi,\,z,\,p)\,] \\[4pt] \dot{w}\,(x,\,z,\,t) = L^{-1}\cdot F^{-1}\,[\,p\bar{w}\,(\xi,\,z,\,p)\,] \end{cases} \tag{1.29}$$

I. 7 Evaluation of the inverse transformations

There will be three ways to evaluate these double inverse transformations. (1) One method is to perform Fourier inversion first, and then do Laplace inversion. This will correspond to Lapwood's method[18], since integral presentation of the periodic wave solution will correspond to the inverse Fourier transformation, and operation of pulse forming will correspond to the inverse Laplace transformation. (2) Another method is to convert Fourier inversion integral to the form of Laplace transformation integral. This will be a logical way of Cagniard's method[3]. (3) Another method is to change the order of integration; first perform Laplace inversion and then do Fourier inversion. This may be a logical way of Takeuchi's method[27].

Separation of function of parameter

Integrands of (1.27), (1.28) are function of p and ξ. However, functions of parameter p are separated by introducing a proper conversion of parameter, $\xi = \lambda p$. This makes Laplace inversion formula available. When parameter ξ is converted by $\xi = \lambda p$, (1.27) and (1.28) become

$$\begin{cases} \phi\,(x,\,z,\,t) = L^{-1}\Big[\dfrac{1}{\sqrt{2\pi}}\int_{-\infty}^{\infty}\dfrac{(2\lambda^2+\frac{1}{V_s^2})}{pF(\lambda)}\cdot\bar{f}\cdot e^{-p(i\lambda x+\sqrt{\lambda^2+\frac{1}{V_p^2}}\,z)}\,d\lambda\Big] \\[14pt] \psi\,(x,\,z,\,t) = L^{-1}\Big[\dfrac{1}{\sqrt{2\pi}}\int_{-\infty}^{\infty}\dfrac{2i\lambda\sqrt{\lambda^2+\frac{1}{V_p^2}}}{pF(\lambda)}\cdot\bar{f}\cdot e^{-p(i\lambda x+\sqrt{\lambda^2+\frac{1}{V_s^2}}\,z)}\,d\lambda\Big] \end{cases} \tag{1.30}$$

and

$$\begin{aligned} u\,(x,\,z,\,t) = L^{-1}\Big[\dfrac{1}{\sqrt{2\pi}}\int_{-\infty}^{\infty}d\lambda\,\Big\{ &\dfrac{(2\lambda^2+\frac{1}{V_s^2})}{F(\lambda)}\cdot\bar{f}\cdot(-i\lambda)\ e^{-p(i\lambda x+\sqrt{\lambda^2+\frac{1}{V_p^2}}\,z)} \\[8pt] &+\dfrac{2i\lambda\sqrt{\lambda^2+\frac{1}{V_p^2}}}{F(\lambda)}\cdot\bar{f}\cdot(-\sqrt{\lambda^2+\frac{1}{V_s^2}}\,)\ e^{-p(i\lambda x+\sqrt{\lambda^2+\frac{1}{V_s^2}}\,z)}\Big\} \end{aligned} \tag{1.31}$$

$$w(x, z, t) = L^{-1}\Big[\frac{1}{\sqrt{2\pi}}\int_{-\infty}^{\infty} d\lambda\Big\{\frac{(2\lambda^2 + \frac{1}{V_s^2})}{F(\lambda)}\cdot \bar{f}\cdot(-\sqrt{\lambda^2 + \frac{1}{V_p^2}})\ e^{-p(i\lambda x + \sqrt{\lambda^2 + \frac{1}{V_p^2}}\,z)}$$

$$+\ \frac{2i\lambda\sqrt{\lambda^2 + \frac{1}{V_p^2}}}{F(\lambda)}\cdot \bar{f}\cdot(i\lambda)\ e^{-p(i\lambda x + \sqrt{\lambda^2 + \frac{1}{V_s^2}}\,z)}\Big\}$$

$$F(\xi, p) = p^4 F(\lambda) = p^4\cdot\mu\Big[(2\lambda^2 + \frac{1}{V_s^2}) - 4\lambda^2\sqrt{\lambda^2 + \frac{1}{V_s^2}}\cdot\sqrt{\lambda^2 + \frac{1}{V_p^2}}\Big]\ . \quad (1.32)$$

It is seen that the integrands of these solutions contain function of p with forms of

$$\frac{1}{p}\,\bar{f}(\lambda, p)\ e^{-p\tau} \qquad \text{for potential solution}$$

$$\bar{f}(\lambda, p)\ e^{-p\tau} \qquad \text{for displacement solution}$$

$$p\bar{f}(\lambda, p)\ e^{-p\tau} \qquad \text{for velocity solution.}$$

When the $\bar{f}(\lambda, p)$ takes such a form that the final integrand does not contain a function of p except the exponential term, the Laplace inversion results in a δ-function. Integration of a function which involves δ-function does not require integral computation. Therefore, if we select either potential solution or displacement solution or velocity solution according to the form of surface force, we can lead the integral to a closed form.

Surface force

By now the surface force has been kept in a general form. Let us give various forms to it. When the surface force $f(x, t)$ is given by a product of a spacial function of x, $f_1(x)$, and a time function $f_2(t)$; i. e.

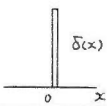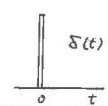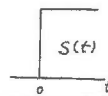$$f(x, t) = f_1(x)\cdot f_2(t)\ , \qquad\qquad (1.33)$$
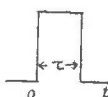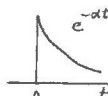
Table I Concentrated force

Type	Spacial component $f_1(x)$	Time component $f_2(t)$	$f_1(x)$	$f_2(t)$	L-F Transform $\bar{f}(\xi, p) = \bar{f_1}(\xi)\,\bar{f_2}(p)$
A I	$x \neq 0 \quad 0$ $x = 0 \quad \infty$ $\delta(x)$	$t < 0 \quad 0$ $t = 0 \quad \infty$ $t > 0 \quad 0$ $\delta(t)$	$\delta(x)$	$\delta(t)$	1
A II	"	$t < 0 \quad 0$ $t > 0 \quad 1$ $S(t)$	"	$S(t)$	$\dfrac{1}{p}$
A III	"	$t < 0 \quad 0$ $0 < t < \tau \quad 1$ $t > \tau \quad 0$ $S(t) - S(t-\tau)$	"		$\dfrac{1}{p}(1 - e^{-p\tau})$
A IV	"	$t < 0 \quad 0$ $0 < t \quad e^{-\alpha t}$	"	$e^{-\alpha t}$	$\dfrac{1}{p + \alpha}$

Table II Spacial force

TYPE	$f_1(x)$	$f_2(t)$	$f_1(x)$	$f_2(t)$	$\bar{f}(\xi,p) = \bar{f}_1(\xi)\,\bar{f}_2(p)$
B I	$-a>x$ 0 $-a<x<a$ $\sqrt{\pi/2}$ $a<x$ 0	$\delta(t)$	(rectangle from $-a$ to a)	$\delta(t)$	$\dfrac{2\sin(\xi a)}{\xi}\cdot 1 = \dfrac{e^{+i\lambda pa}-e^{-i\lambda pa}}{i\lambda p}$
B II	"	$S(t)$	"	$S(t)$	$\dfrac{2\sin(\xi a)}{\xi}\cdot\dfrac{1}{p} = \dfrac{e^{+i\lambda pa}-e^{-i\lambda pa}}{i\lambda p^2}$
B III	"	$S(t)-S(t-\tau)$	"	(step of width τ)	$\dfrac{2\sin(\xi a)}{\xi}\cdot\dfrac{1}{p}(1-e^{-p\tau})$ $= \dfrac{e^{i\lambda pa}-e^{-i\lambda pa}}{i\lambda p^2}(1-e^{-p\tau})$
B IV	"	$t<0$ 0 $0<t$ $e^{-\alpha t}$	"	$e^{-\alpha t}$	$\dfrac{2\sin(\xi a)}{\xi}\cdot\dfrac{1}{p+\alpha}$ $= \dfrac{e^{i\lambda pa}-e^{-i\lambda pa}}{i\lambda p(p+\alpha)}$

the Laplace-Fourier transforms of various surface forces are obtained as shown in Tables I and II. Table I shows concentrated force at the origin and Table II shows spacial force.

From the above tables, we can select a type of solution which results in a closed form ; displacement solution for AI type surface force, velocity solution for AII, AIII and BI types, and acceleration solution for BII and BIII types. AIV and BIV types will not have suitable solution. Moreover we can see that the displacement solution for AI type is equal to the velocity solution for AII type, and the velocity solution for BI type is equal to the acceleration solution for BII type. This means that the difference of the δ-function type and the step-function type of the surface force is not the essential difference for the generation of the elastic waves. The difference between a concentrated force and a spacial force is essential because of additional factor $\dfrac{1}{i\lambda}$ for the spacial force.

In the following sections, we perform the evaluations for the AI, AII type forces and for the BI, BII type forces.

Final evaluation for a concentrated force at the origin

Let us make the final evaluation for the concentrated force at the origin. We take the displacement solution for the AI type force. This solution is equal to the velocity solution for the AII type.

Laplace-Fourier transform of the AI type force is, from the above Table I,

$$\bar{f}(\xi, p) = 1 \tag{1.34}$$

By putting (1.34) into (1.31) (1.32), we get the displacement solution ;

$$u(x, z, t) = L^{-1}\frac{1}{\sqrt{2\pi}}\int_{-\infty}^{\infty}\left\{ iG_1(\lambda)\,e^{-p\tau_1} + iG_2(\lambda)\,e^{-p\tau_2} \right\}\,d\lambda \tag{1.35}$$

$$w(x, z, t) = L^{-1}\frac{1}{\sqrt{2\pi}}\int_{-\infty}^{\infty}\left\{ G_3(\lambda)\,e^{-p\tau_1} + G_4(\lambda)\,e^{-p\tau_2} \right\}\,d\lambda \tag{1.36}$$

where

$$
\begin{cases}
G_1(\lambda) = - \dfrac{\lambda}{F(\lambda)} \left(2\lambda^2 + \dfrac{1}{V_s^2} \right) \\[2mm]
G_2(\lambda) = - \dfrac{2\lambda}{F(\lambda)} \sqrt{\lambda^2 + \dfrac{1}{V_p^2}} \sqrt{\lambda^2 + \dfrac{1}{V_s^2}} \\[2mm]
G_3(\lambda) = - \dfrac{1}{F(\lambda)} \left(2\lambda^2 + \dfrac{1}{V_s^2} \right) \sqrt{\lambda^2 + \dfrac{1}{V_p^2}} \\[2mm]
G_4(\lambda) = - \dfrac{1}{F(\lambda)} \left(2\lambda^2 \sqrt{\lambda^2 + \dfrac{1}{V_p^2}} \right)
\end{cases}
\tag{1.37}
$$

$$
F(\lambda) = \mu \left[\left(2\lambda^2 + \dfrac{1}{V_s^2} \right)^2 - 4\lambda^2 \sqrt{\lambda^2 + \dfrac{1}{V_s^2}} \sqrt{\lambda^2 + \dfrac{1}{V_p^2}} \right]
\tag{1.38}
$$

$$
\begin{cases}
\tau_1 = i\lambda x + \sqrt{\lambda^2 + \dfrac{1}{V_p^2}}\, z \\[2mm]
\tau_2 = i\lambda x + \sqrt{\lambda^2 + \dfrac{1}{V_s^2}}\, z \quad .
\end{cases}
\tag{1.39}
$$

$G_1(\lambda)$ and $G_2(\lambda)$ are odd functions of λ and $G_3(\lambda)$, $G_4(\lambda)$ and a part of exponential term are even functions of λ. Also we have $e^{-i\lambda p x} = \cos p\lambda x - i \sin p\lambda x$. Therefore, integration from the negative infinity to the positive infinity with respect to λ, becomes a real or imaginary part of the integration from zero to the positive infinity,

$$
\begin{cases}
u(x, z, t) = L^{-1} \cdot - \sqrt{\dfrac{2}{\pi}}\, I_m \displaystyle\int_0^\infty \left\{ G_1(\lambda)\, e^{-p\tau_1} + G_2(\lambda)\, e^{-p\tau_2} \right\}\, d\lambda \\[4mm]
w(x, z, t) = L^{-1} \sqrt{\dfrac{2}{\pi}}\, R_e \displaystyle\int_0^\infty \left\{ G_3(\lambda)\, e^{-p\tau_1} + G_4(\lambda)\, e^{-p\tau_2} \right\}\, d\lambda \quad .
\end{cases}
\tag{1.40}
$$

Unless we change the range of integration, we must take into account the complicated behavior on Riemman surface. Now we change the order of integration. Performing Laplace inverse transformation, we get

$$
\begin{cases}
u(x, z, t) = - \sqrt{\dfrac{2}{\pi}}\, I_m \displaystyle\int_0^\infty \left\{ G_1(\lambda)\, \delta(t - \tau_1) + G_2(\lambda)\, \delta(t - \tau_2) \right\}\, d\lambda \\[4mm]
w(x, z, t) = \sqrt{\dfrac{2}{\pi}}\, R_e \displaystyle\int_0^\infty \left\{ G_3(\lambda)\, \delta(t - \tau_1) + G_4(\lambda)\, \delta(t - \tau_2) \right\}\, d\lambda \quad .
\end{cases}
\tag{1.41}
$$

Because argument of δ-function involves τ_1 and τ_2 which are function of λ, we change the integration parameter λ to τ. Thus we get

$$
\begin{cases}
u(x, z, t) = - \sqrt{\dfrac{2}{\pi}} I_m \left\{ \displaystyle\int_{L_1} G_1(\lambda)\, \delta(t - \tau_1) \dfrac{\partial \lambda}{\partial \tau_1} d\tau_1 + \displaystyle\int_{L_2} G_2(\lambda)\, \delta(t - \tau_2) \dfrac{\partial \lambda}{\partial \tau_2} d\tau_2 \right\} \\[4mm]
w(x, z, t) = \sqrt{\dfrac{2}{\pi}} R_e \left\{ \displaystyle\int_{L_1} G_3(\lambda)\, \delta(t - \tau_1) \dfrac{\partial \lambda}{\partial \tau_1} d\tau_1 + \displaystyle\int_{L_2} G_4(\lambda)\, \delta(t - \tau_2) \dfrac{\partial \lambda}{\partial \tau_2} d\tau_2 \right\}
\end{cases}
\tag{1.42}
$$

where

$$
\begin{cases}
\dfrac{\partial \lambda}{\partial \tau_{1,2}} = \dfrac{1}{x^2 + z^2} \left\{ -ix + \dfrac{z\tau}{\sqrt{\tau^2 - \dfrac{x^2 + z^2}{V_{p,s}^2}}} \right\}
\end{cases}
\tag{1.43}
$$

$$\left. \right\} \lambda = \frac{1}{x^2 + z^2} \left\{ - ix\tau + z \sqrt{\tau^2 - \frac{x^2 + z^2}{V_{p,s}^2}} \right\} \quad .$$

L_1 and L_2 are the integration path on the τ-plane corresponding to the positive real axis on the λ-plane.

The transformation from the λ-plane to τ-plane is well described in Garvin's paper[8].
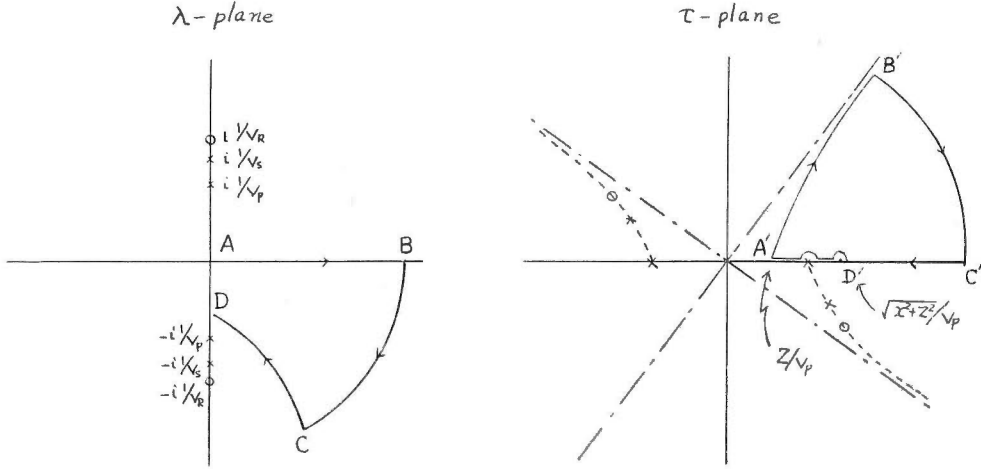

Fig. 2

Imaginary axis of the λ-plane is transformed to the dotted line on the τ-plane, on which are a pole and branch points of the integrand. The positive real axis of the λ-plane is transformed to the line A'B' on the τ-plane. Therefore, path L is the line A'B'.

Since t is a real time, we have to add another path on the real axis of the τ-plane. We add path B'C'D'A' on the τ-plane, as shown in Fig. 2, forming a closed path within which there are neither pole nor singular points. Corresponding path BCDA on the λ-plane is also shown in Fig. 2, where DA is on the imaginary axis of λ-plane. Then we can evaluate the integral (1.42) by Cauchy's theorem ;

$$\int_{L_1} \equiv \int_{A'B'} = - \int_{B'C'} - \int_{C'D'} - \int_{D'A} \quad . \tag{1.44}$$

The integral on the segment B'C' vanishes because of large value of τ—large value of λ and $G(\lambda) \propto \frac{1}{\lambda}$. On the segment D'A', λ and $\frac{\partial \lambda}{\partial \tau}$ become purely imaginary. Also $G_1(\lambda)$ and $G_2(\lambda)$ become purely imaginary, while $G_3(\lambda)$ and $G_4(\lambda)$, functions of λ^2, become real. Therefore, there are no imaginary part in the integrand of $u(x, z, t)$, and also no real part in the integrand of $w(x, z, t)$. Thus the integration on the path D'A' vanishes. Finally we get

$$\int_{A'B'} = - \int_{C'D'} = \int_{D'C'} \quad . \tag{1.45}$$

Because of $\delta(t-\tau)$ function, in which both t and τ are real on the segment of path, $D'C'$, we get the final expression for the displacement solution,

$$\begin{cases} u(x,z,t) = -\sqrt{\dfrac{2}{\pi}}\, I_m\left[G_1(\lambda)\dfrac{\partial\lambda}{\partial\tau_1}\Big|_{t=\tau_1} + G_2(\lambda)\dfrac{\partial\lambda}{\partial\tau_2}\Big|_{t=\tau_2}\right] \\[4mm] w(x,z,t) = \sqrt{\dfrac{2}{\pi}}\, R_e\left[G_3(\lambda)\dfrac{\partial\lambda}{\partial\tau_1}\Big|_{t=\tau_1} + G_4(\lambda)\dfrac{\partial\lambda}{\partial\tau_2}\Big|_{t=\tau_2}\right] \end{cases} \quad (1.46)$$

$$\tau_1 > \sqrt{x^2+z^2}/V_p, \quad \tau_2 > \sqrt{x^2+z^2}/V_s$$

where $G_l(\lambda)$ and $\dfrac{\partial\lambda}{\partial\tau_l}$ are given in (1.37) and (1.43).

These are the solutions in the subsurface. In the special cases they are simplified as follows.

(i) Solutions on the surface are obtained by putting λ and $\dfrac{\partial\lambda}{\partial\tau}$ to

$$\begin{cases} \tau_1 = \tau_2 = i\lambda x \\[2mm] \lambda = -i\tau/x \\[2mm] \dfrac{d\lambda}{d\tau} = -i/x \end{cases} \quad (1.47)$$

(ii) Solutions on the vertical axis are obtained by putting λ and $\dfrac{\partial\lambda}{\partial\tau}$ to

$$\begin{cases} \tau_1 = \sqrt{\lambda^2 + \dfrac{1}{V_p^2}}\, z \\[4mm] \tau_2 = \sqrt{\lambda^2 + \dfrac{1}{V_s^2}}\, z \end{cases} \quad (1.48)$$

and

$$\begin{cases} \lambda = \dfrac{1}{z}\sqrt{\tau^2 - \dfrac{z^2}{V_{p,s}^2}} \\[4mm] \dfrac{\partial\lambda}{\partial\tau} = \dfrac{1}{z}\dfrac{\tau}{\sqrt{\tau^2 - \dfrac{z^2}{V_{p,s}^2}}} \end{cases} \quad (1.49)$$

Final evaluation for a spacial force

We evaluate the velocity solution for the BI type force. This solution is equal to the acceleration solution for BII type. The Laplace-Fourier transform of the BI type force is, from the Table II,

$$\bar{f}(\lambda,p) = \dfrac{e^{i\lambda pa} - e^{-i\lambda pa}}{i\lambda p} \quad . \quad (1.50)$$

Velocity solution is obtained by putting (1.50) into (1.29)

$$\begin{cases} \dot{u}(x,z,t) = L^{-1}\dfrac{1}{\sqrt{2\pi}}\int_{-\infty}^{\infty} d\lambda\left\{G_1(\lambda)\,e^{-p\tau_1} - G_1(\lambda)\,e^{-p\tau_2} + G_2(\lambda)\,e^{-p\tau_3} - G_2(\lambda)\,e^{-p\tau_4}\right\} \\[4mm] \dot{w}(x,z,t) = L^{-1}\dfrac{1}{\sqrt{2\pi}}\int_{-\infty}^{\infty} d\lambda\left\{iG_3(\lambda)e^{-p\tau_1} - iG_3(\lambda)e^{-p\tau_2} + iG_4(\lambda)e^{-p\tau_3} - iG_4(\lambda)e^{-p\tau_4}\right\} \end{cases} \quad (1.51)$$

12

where

$$
\begin{cases}
\tau_1 = i\lambda(x+a) + \sqrt{\lambda^2 + \dfrac{1}{V_p{}^2}}\ z \\[2mm]
\tau_2 = i\lambda(x-a) + \sqrt{\lambda^2 + \dfrac{1}{V_p{}^2}}\ z \\[2mm]
\tau_3 = i\lambda(x+a) + \sqrt{\lambda^2 + \dfrac{1}{V_s{}^2}}\ z \\[2mm]
\tau_4 = i\lambda(x-a) + \sqrt{\lambda^2 + \dfrac{1}{V_s{}^2}}\ z
\end{cases}
\tag{1.52}
$$

$$
\begin{cases}
G_1(\lambda) = -\dfrac{1}{F(\lambda)}\left(2\lambda^2 + \dfrac{1}{V_s{}^2}\right) \\[2mm]
G_2(\lambda) = -\dfrac{1}{F(\lambda)} 2\sqrt{\lambda^2 + \dfrac{1}{V_p{}^2}}\sqrt{\lambda^2 + \dfrac{1}{V_s{}^2}} \\[2mm]
G_3(\lambda) = +\dfrac{1}{F(\lambda)}\left(2\lambda^2 + \dfrac{1}{V_s{}^2}\right)\sqrt{\lambda^2 + \dfrac{1}{V_p{}^2}}\cdot\dfrac{1}{\lambda} \\[2mm]
G_4(\lambda) = +\dfrac{1}{F(\lambda)}(2\lambda)\sqrt{\lambda^2 + \dfrac{1}{V_p{}^2}}\ .
\end{cases}
\tag{1.53}
$$

We follow the same procedure of evaluation described in the preceding section; change the integration range, change the order of integration and convert λ-plane to τ-plane. Then, we finally get the velocity solution for the spacial force,

$$
\begin{cases}
\bar{\dot{u}}(x,z,t) = \sqrt{\dfrac{2}{\pi}}\ R_e\left\{G_1(\lambda)\dfrac{\partial\lambda}{\partial\tau_1}\Big|_{t=\tau_1} -G_1(\lambda)\dfrac{\partial\lambda}{\partial\tau_2}\Big|_{t=\tau_2} +G_2(\lambda)\dfrac{\partial\lambda}{\partial\tau_3}\Big|_{t=\tau_3} -G_2(\lambda)\dfrac{\partial\lambda}{\partial\tau_4}\Big|_{t=\tau_4}\right\} \\[3mm]
\bar{\dot{w}}(x,z,t) = \sqrt{\dfrac{2}{\pi}}\ I_m\left\{G_3(\lambda)\dfrac{\partial\lambda}{\partial\tau_1}\Big|_{t=\tau_1} -G_3(\lambda)\dfrac{\partial\lambda}{\partial\tau_2}\Big|_{t=\tau_2} +G_4(\lambda)\dfrac{\partial\lambda}{\partial\tau_3}\Big|_{t=\tau_3} -G_4(\lambda)\dfrac{\partial\lambda}{\partial\tau_4}\Big|_{t=\tau_4}\right\}
\end{cases}
\tag{1.54}
$$

where $G_i(\lambda)$ and τ_i are given in (1.52) and (1.53).

The first and second terms are contributions from a dilatational wave component, and the third and fourth terms are contributions from an equivoluminal wave component. These terms will reveal the effect of pattern shooting for the reduction of surface waves, when numerical computation will be made. Solutions in the special cases will be easily obtained in a similar way of the preceding section.

II. Buried Line Source Problem

II. 1 Introduction

Propagation of a transient elastic wave generated by an internal source in a semi-infinite elastic medium has been studied by many investigators; Nakano[19], Sakai[20], Lapwood[18], Takeuchi and Kabayashi[26], Dix[6] and Garvin[8]. The exact solution at the surface of a medium is already presented and also mechanism of generation of Rayleigh wave is fully established.

In this chapter, mathematical expression for solving the problem is rewritten in a simple form by the method of integral transformation. By this

expression, selection of the source function and Cagniard's technique of inverse transformation will be easily understood. A comparison of this method and other methods is briefly discussed in the last section II. 4.

II. 2 Formal solutions

Let us take x-y axes on the surface of the elastic medium and z-axis vertically downward into the medium. A line source is placed in a medium at $z=f$, $x=0$. We assume the motion of an elastic medium is two dimensional. Then Laplace-Fourier transformed wave equations are, from (1.7)
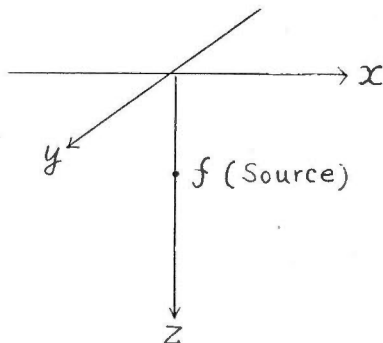
Fig. 3

$$\begin{cases} \dfrac{d^2\phi}{dz^2} - (\xi^2 + h^2)\,\bar{\phi} = 0 \\[2mm] \dfrac{d^2\bar{\phi}}{dz^2} - (\xi^2 + k^2)\,\bar{\phi} = 0 \end{cases} \tag{2.1}$$

Laplace-Fourier transformed boundary conditions to be satisfied at the surface $z=0$, are

$$\begin{cases} [\bar{P}_{zz}]_{z=0} = -\lambda\xi\bar{\phi} + (\lambda + 2\mu)\,\bar{\phi}_{zz} + 2i\mu\xi\bar{\psi}_z = 0 \\[2mm] [\bar{P}_{xz}]_{z=0} = \mu\,(-2i\xi\bar{\phi}_z + \bar{\psi}_{zz} + \xi^2\bar{\psi}) = 0 \end{cases} \tag{2.2}$$

Solutions of wave equations (2.1) consist of a general solution and a particular solution which presents a source function. Taking a dilatational line source, we have, in the transformed space,

$$\bar{\phi}_0\,(\xi, z, p) = A_0\,(p, \xi)\,e^{-\sqrt{\xi^2+h^2}(f-z)} \tag{2.3}$$

where $A_0\,(\xi, p)$ will be determined later by a source condition.
Thus, we have solutions of the wave equations (2.1),

$$\begin{cases} \bar{\phi} = \bar{\phi}_0 + \bar{\phi}_1 \\ \bar{\psi} = \bar{\psi}_1 \end{cases} \tag{2.4}$$

where

$$\begin{cases} \bar{\phi}_1 = A\,(\xi, p)\,e^{-\sqrt{\xi^2+h^2}\,z} \\[2mm] \bar{\psi}_1 = B\,(\xi, p)\,e^{-\sqrt{\xi^2+k^2}\,z} \end{cases} \tag{2.5}$$

14

$A(\xi, p)$ and $B(\xi, p)$ are determined by putting (2.4) (2.5) into (2.2);

$$
\begin{cases}
A(\xi, p) = -A_0\, e^{-\sqrt{\xi^2+h^2}\,f} - \dfrac{A_0}{F(\xi, p)}\, e^{-\sqrt{\xi^2+k^2}\,f}\, \mu\,(8\xi^2\,\sqrt{\xi^2+k^2}\,\sqrt{\xi^2+h^2}) \\[2mm]
B(\xi, p) = \dfrac{A_0}{F(\xi, p)}\, e^{-\sqrt{\xi^2+h^2}\,f}\, \mu\{\, 2(2\xi^2 + k^2)\, i\xi\sqrt{\xi^2+h^2}\,\}
\end{cases}
\tag{2.6}
$$

where

$$
F(\xi, p) = \mu\{\,(2\xi^2 + k^2)^2 - 4\xi^2\,\sqrt{\xi^2+h^2}\sqrt{\xi^2+k^2}\,\} \quad .
\tag{2.7}
$$

Formal potential solutions in the Laplace-Fourier transformed space are

$$
\begin{aligned}
\bar{\phi}(\xi, z, p) =\ & A_0(\xi, p)\, e^{-\sqrt{\xi^2+h^2}(f-z)} \\
& - A_0(\xi, p)\, e^{-\sqrt{\xi^2+h^2}(f+z)} \\
& - \frac{A_0(\xi, p)}{F(\xi, p)}\, \mu\,(8\xi^2\sqrt{\xi^2+h^2}\,\sqrt{\xi^2+k^2})\, e^{-\sqrt{\xi^2+h^2}(f+z)}
\end{aligned}
\tag{2.8}
$$

$$
\bar{\varphi}(\xi, z, p) = \frac{A_0(\xi, p)}{F(\xi, p)}\, \mu\{\, 2(2\xi^2 + k^2)\, i\xi\sqrt{\xi^2+h^2}\,\}\, e^{-(\sqrt{\xi^2+h^2}\,f + \sqrt{\xi^2+k^2}\,z)} \quad .
\tag{2.9}
$$

Thus, formal potential solutions in the original space (x, z, t) are

$$
\begin{cases}
\phi(x, z, t) = L^{-1} \cdot F^{-1}\,\{\, \bar{\phi}(\xi, z, p)\,\} \\
\varphi(x, z, t) = L^{-1} \cdot F^{-1}\,\{\, \bar{\varphi}(\xi, z, p)\,\} \quad,
\end{cases}
\tag{2.10}
$$

where L^{-1} and F^{-1} denote the operation of Laplace inversion integral and Fourier inversion integral respectively,

$$
\begin{cases}
L^{-1} \equiv \dfrac{1}{2\pi j} \displaystyle\int_{c-j\infty}^{c+j\infty} e^{pt}\, dp, \\[3mm]
F^{-1} \equiv \dfrac{1}{\sqrt{2\pi}} \displaystyle\int_{-\infty}^{\infty} e^{-i\xi x}\, dx \quad .
\end{cases}
\tag{2.11}
$$

Formal displacement solutions in the Laplace-Fourier transformed space are obtained from the relations

$$
\begin{cases}
\bar{u} = -i\xi\bar{\phi} + \bar{\varphi}_z \\
\bar{w} = \bar{\phi}_z + i\xi\bar{\varphi} \quad .
\end{cases}
\tag{2.12}
$$

Thus, we have

$$
\begin{aligned}
\bar{u} =\ & -i\xi A_0 \exp\{\,-(f-z)\sqrt{\xi^2+h^2}\,\} \\
& + i\xi A_0 \exp\{\,-(f+z)\sqrt{\xi^2+h^2}\,\} \\
& + \frac{i\xi A_0}{F(\xi, p)}\, \{\, 8\xi^2\sqrt{\xi^2+h^2}\,\sqrt{\xi^2+k^2}\,\}\, \exp\{\,-(f+z)\sqrt{\xi^2+h^2}\,\} \\
& - \frac{A_0\mu}{F(\xi, p)}\, \sqrt{\xi^2+k^2}\,\{\, 2(2\xi^2 + k^2)\, i\xi\sqrt{\xi^2+h^2}\,\} \\
& \qquad\qquad \exp\{\,-f\sqrt{\xi^2+h^2}\,\}\, \exp\{\,-z\sqrt{\xi^2+k^2}\,\} \\
\equiv\ & \bar{u}_0 + \bar{u}_{10} + \bar{u}_{11} + \bar{u}_2
\end{aligned}
\tag{2.13}
$$

$$\bar{w} = \sqrt{\xi^2 + h^2}\, A_0 \exp\{-(f-z)\sqrt{\xi^2 + h^2}\}$$
$$+ \sqrt{\xi^2 + h^2}\, A_0 \exp\{-(f+z)\sqrt{\xi^2 + h^2}\}$$
$$+ \frac{A_0\mu}{F(\xi, p)}\sqrt{\xi^2 + h^2}\,\{8\xi^2\sqrt{\xi^2 + h^2}\sqrt{\xi^2 + k^2}\}\exp\{-(f+z)\sqrt{\xi^2 + h^2}\}$$
$$- \frac{A_0\mu}{F(\xi, p)}\,\xi^2\{2(2\xi^2 + k^2)\sqrt{\xi^2 + h^2}\}\exp\{-f\sqrt{\xi^2 + h^2}\}\exp\{-z\sqrt{\xi^2 + k^2}\}$$
$$\equiv \bar{w}_0 + \bar{w}_{10} + \bar{w}_{11} + \bar{w}_2 \quad . \tag{2.14}$$

$\bar{u}_0$ and $\bar{w}_0$ are components of the source wave. $\bar{u}_{10}$, $\bar{u}_{11}$, $\bar{w}_{10}$, $\bar{w}_{11}$ are the dilatational components derived from $\bar{\phi}_1$. $\bar{u}_2$ and $\bar{w}_2$ are the equi-voluminal components derived from $\bar{\phi}_1$. $\bar{u}_{10}$ and $\bar{w}_{10}$ are interpreted as contributions from the perfect image source, and $\bar{u}_{11}$, $\bar{w}_{11}$ are interpreted as the correction to the perfect image source reflection due to the conversion from dilatational wave to equivoluminal wave at the surface. Formal displacement solutions in the original space are

$$\begin{cases} u(x, z, t) = L^{-1} \cdot F^{-1}\{\bar{u}(\xi, z, p)\} \\ w(x, z, t) = L^{-1} \cdot F^{-1}\{\bar{w}(\xi, z, p)\} \end{cases} \tag{2.15}$$

II. 3 Evaluation of the inverse transformations

Separation of a function of parameter p

We follow the same steps for the evaluation of the inverse transformation as that of the surface force problem. We separate a function of p in the integrand of the inverse transformation integral by converting ξ to λp. Then we get,

$$\begin{cases} u(x, z, t) = u_0 + u_{10} + u_{11} + u_2 \\ w(x, z, t) = w_0 + w_{10} + w_{11} + w_2 \end{cases} \tag{2.16}$$

$$\begin{cases} u_0 = L^{-1} \cdot \frac{1}{\sqrt{2\pi}} \int_{-\infty}^{\infty} d\lambda\,\{-i\lambda p^2\, A_0 \exp(-p\tau_1)\} \\[2mm] u_{10} = L^{-1} \cdot \frac{1}{\sqrt{2\pi}} \int_{-\infty}^{\infty} d\lambda\,\{i\lambda p^2\, A_0 \exp(-p\tau_2)\} \\[2mm] u_{11} = L^{-1} \cdot \frac{1}{\sqrt{2\pi}} \int_{-\infty}^{\infty} d\lambda\,\{\frac{A_0\mu}{F(\lambda, p)} i\lambda p^6 \sqrt{\lambda^2 + \frac{1}{V_p^2}}\sqrt{\lambda^2 + \frac{1}{V_s^2}} 8\lambda^2 \exp(-p\tau_2)\} \\[2mm] u_2 = L^{-1} \cdot \frac{1}{\sqrt{2\pi}} \int_{-\infty}^{\infty} d\lambda\,\{-\frac{A_0\mu}{F(\lambda, p)} i\lambda p^6 \sqrt{\lambda^2 + \frac{1}{V_p^2}}\sqrt{\lambda^2 + \frac{1}{V_s^2}} 2(2\lambda^2 + \frac{1}{V_s^2})\exp(-p\tau_3)\} \end{cases} \tag{2.17}$$

$$\begin{cases} w_0 = L^{-1} \cdot \frac{1}{\sqrt{2\pi}} \int_{-\infty}^{\infty} d\lambda\,\{p^2\sqrt{\lambda^2 + \frac{1}{V_p^2}}\, A_0 \exp(-p\tau_1)\} \\[2mm] w_{10} = L^{-1} \cdot \frac{1}{\sqrt{2\pi}} \int_{-\infty}^{\infty} d\lambda\,\{p^2\sqrt{\lambda^2 + \frac{1}{V_p^2}}\, A_0 \exp(-p\tau_2)\} \\[2mm] w_{11} = L^{-1} \cdot \frac{1}{\sqrt{2\pi}} \int_{-\infty}^{\infty} d\lambda\,\{\frac{A_0\mu}{F(\lambda, p)} p^6 \lambda^2 \sqrt{\lambda^2 + \frac{1}{V_p^2}} 8\sqrt{\lambda^2 + \frac{1}{V_p^2}}\sqrt{\lambda^2 + \frac{1}{V_s^2}} \exp(-p\tau_2)\} \\[2mm] w_2 = L^{-1} \cdot \frac{1}{\sqrt{2\pi}} \int_{-\infty}^{\infty} d\lambda\,\{-\frac{A_0\mu}{F(\lambda, p)} p^6 \lambda^2 \sqrt{\lambda^2 + \frac{1}{V_p^2}} 2(2\lambda^2 + \frac{1}{V_s^2})\exp(-p\tau_3)\} \end{cases} \tag{2.18}$$

$$F(\lambda, p) \equiv p^4 F(\lambda) = \mu p^4 \left[\left\{ 2\lambda^2 + \frac{1}{V_s^2} \right\}^2 - 4\lambda^2 \sqrt{\lambda^2 + \frac{1}{V_p^2}} \sqrt{\lambda^2 + \frac{1}{V_s^2}} \right]$$

$$(2.19)$$

$$\begin{cases} \tau_1 = \sqrt{\lambda^2 + \frac{1}{V_p^2}} \, (f - z) + i\lambda x \\[2mm] \tau_2 = \sqrt{\lambda^2 + \frac{1}{V_p^2}} \, (f + z) + i\lambda x \\[2mm] \tau_3 = \sqrt{\lambda^2 + \frac{1}{V_p^2}} \, f + \sqrt{\lambda^2 + \frac{1}{V_s^2}} \, z + i\lambda x \end{cases} \qquad (2.20)$$

We can see the function of parameter p in the integrand has the form of

$$p^2 A_0 (\lambda, p) \, G(\lambda) \, e^{-p\tau} \quad . \tag{2.21}$$

Therefore the integral will go to a closed form when $A_0(\lambda, p)$ takes a form of $f(\lambda)/p^2$, $e^{-p\tau}$ being the only function of p in the integrand. In the next section, let us see forms of source functions.

Source function

It will be easily shown that a particular solution K_0, the modified Bessel function, derived from the Laplace transformed wave equation has the best suit form among many particular solutions. This solution, with a factor $1/p^2$, leads the inverse transformation integral to a closed form. A particular solution of the Laplace transformed equation

$$(\nabla^2 - h^2) \, \Phi (x, z, p) = 0 \tag{2.22}$$

is

$$\Phi_0 = a_0 (p) \, K_0 \left[h\sqrt{x^2 + (f - z)^2} \right] \tag{2.23}$$

where $a_0(p)$ is a arbitrary function of p. Fourier transform of this solution is

$$\bar{\phi}(\xi, z, p) = \sqrt{\frac{\pi}{2}} \, \frac{a_0(p)}{\sqrt{h^2 + \xi^2}} \, e^{-\sqrt{\xi^2 + h^2} \,(f-z)} \quad , \quad f - z > 0. \tag{2.24}$$

When we choose $1/p$ for $a_0(p)$, and covert ξ to λp, we get a expression for A_0 of the source function (2.3),

$$A_0 = \sqrt{\frac{\pi}{2}} \cdot \frac{1}{p} \cdot \frac{1}{\sqrt{\xi^2 + h^2}} = \sqrt{\frac{\pi}{2}} \cdot \frac{1}{p^2} \cdot \frac{1}{\sqrt{\lambda^2 + \frac{1}{V_p^2}}} \quad . \tag{2.25}$$

The source function in the original space is obtained by performing inverse Laplace transformation to (2.23),

$$\phi_0 (x, z, t) = \begin{cases} 0 & \text{for } t < r/V_p \\ \cosh^{-1} t/r/V_p & \text{for } t > r/V_p \end{cases} \tag{2.26}$$

where

$$r = \sqrt{x^2 + (f - z)^2} \quad .$$

The displacement u_{or} in the outgoing direction of this source wave is

$$u_{or} = \frac{\partial \phi_0}{\partial r} = - \frac{t}{r\sqrt{t^2 - (r/V_p)^2}} \qquad (2.27)$$

$$= - \frac{\tau}{r\sqrt{\tau^2 - 1}} \qquad (2.27)'$$

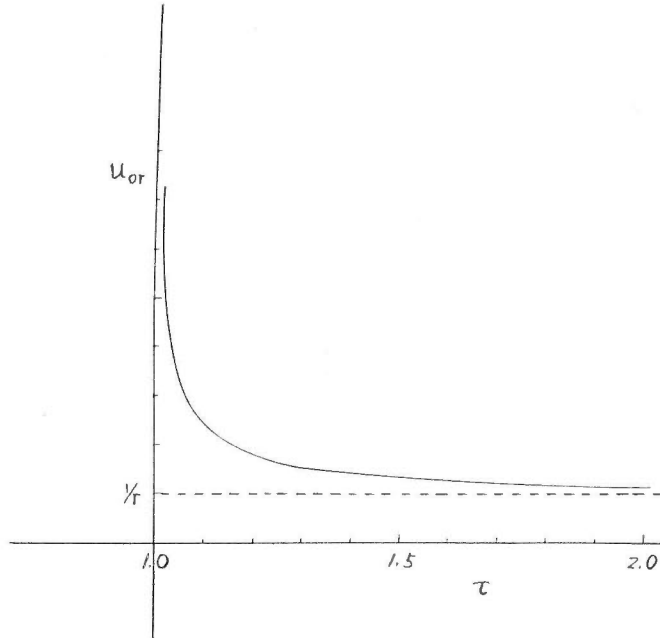where $\tau = t/t_0$, $t_0 = r/V_p$. The form of u_{or} is shown in Fig. 4.

Fig. 4. Displacement wave form of the source wave

This source function is the same one as used by Lapwood[18] and Garvin[8].

Final evaluation

Since we gave a form to a source function, we now perform the final evaluation. By putting A_0 into (2.17) (2.18), we get the expression for the displacement solution,

$$
\begin{aligned}
u(x, z, t) = L^{-1} \cdot \frac{1}{2} \int_{-\infty}^{\infty} d\lambda \{ &- iG_0(\lambda) \exp(-p\tau_1) \\
&+ iG_0(\lambda) \exp(-p\tau_2) \\
&+ iG_1(\lambda) \exp(-p\tau_2) \\
&- iG_2(\lambda) \exp(-p\tau_3) \}
\end{aligned} \qquad (2.28)
$$

$$
\begin{aligned}
w(x, z, t) = L^{-1} \cdot \frac{1}{2} \int_{-\infty}^{\infty} d\lambda \{ &+ \qquad \exp(-p\tau_1) \\
&+ \qquad \exp(-p\tau_2) \\
&+ G_3(\lambda) \exp(-p\tau_2) \\
&- G_4(\lambda) \exp(-p\tau_3) \}
\end{aligned} \qquad (2.29)
$$

18

where

$$
\begin{cases}
G_0(\lambda) = \dfrac{\lambda}{\sqrt{\lambda^2 + \dfrac{1}{V_p{}^2}}} \\[4mm]
G_1(\lambda) = \dfrac{\lambda}{F(\lambda)} \; 8\lambda^2 \sqrt{\lambda^2 + \dfrac{1}{V_s{}^2}} \\[4mm]
G_2(\lambda) = \dfrac{2\lambda}{F(\lambda)} \; (2\lambda^2 + \dfrac{1}{V_s{}^2}) \sqrt{\lambda^2 + \dfrac{1}{V_s{}^2}} \\[4mm]
G_3(\lambda) = \dfrac{8\lambda^2}{F(\lambda)} \sqrt{\lambda^2 + \dfrac{1}{V_p{}^2}} \sqrt{\lambda^2 + \dfrac{1}{V_s{}^2}} \\[4mm]
G_4(\lambda) = \dfrac{2\lambda^2}{F(\lambda)} \; (2\lambda^2 + \dfrac{1}{V_s{}^2})
\end{cases}
\tag{2.30}
$$

$$
\begin{cases}
\tau_1 = \sqrt{\lambda^2 + \dfrac{1}{V_p{}^2}}\;(f - z) + i\lambda x \\[4mm]
\tau_2 = \sqrt{\lambda^2 + \dfrac{1}{V_p{}^2}}\;(f + z) + i\lambda x \\[4mm]
\tau_3 = \sqrt{\lambda^2 + \dfrac{1}{V_p{}^2}}\; f + \sqrt{\lambda^2 + \dfrac{1}{V_s{}^2}}\; z + i\lambda x
\end{cases}
\tag{2.31}
$$

$$
F(\lambda) = \left[(2\lambda^2 + \dfrac{1}{V_s{}^2})^2 - 4\lambda^2 \sqrt{\lambda^2 + \dfrac{1}{V_p{}^2}} \sqrt{\lambda^2 + \dfrac{1}{V_s{}^2}} \right]. \tag{2.32}
$$

We follow the same procedure used in the surface force problem for the further evaluation. The integration with λ from the negative infinity to the positive infinity is simplified to

$$
\begin{cases}
u = L^{-1} \cdot I_m \displaystyle\int_0^\infty - G(\lambda)\, e^{-p\tau}\, d\lambda \\[4mm]
w = L^{-1} \cdot R_e \displaystyle\int_0^\infty G(\lambda)\, e^{-p\tau}\, d\lambda
\end{cases}
$$

because G_0, G_1 and G_2 are odd, and G_3, G_4 are even functions of λ. Then we change the order of integration and perform the inverse Laplace transformation first ;

$$
\begin{cases}
u = - I_m \displaystyle\int_0^\infty G(\lambda)\, \delta(t - \tau)\, d\lambda \\[4mm]
w = R_e \displaystyle\int_0^\infty G(\lambda)\, \delta(t - \tau)\, d\lambda \quad .
\end{cases}
$$

We convert this integration in the λ-plane into the τ-plane because of $\delta(t - \tau)$ function, and we have

$$
\begin{cases}
u = - I_m \displaystyle\int_L G(\lambda)\, \delta(t - \tau)\, \dfrac{\partial \lambda}{\partial \tau}\, d\tau \\[4mm]
w = R_e \displaystyle\int_L G(\lambda)\, \delta(t - \tau)\, \dfrac{\partial \lambda}{\partial \tau}\, d\tau \quad .
\end{cases}
$$

By the same argument made in the surface force problem, this integration goes to the integration along the real axis of the τ-plane.
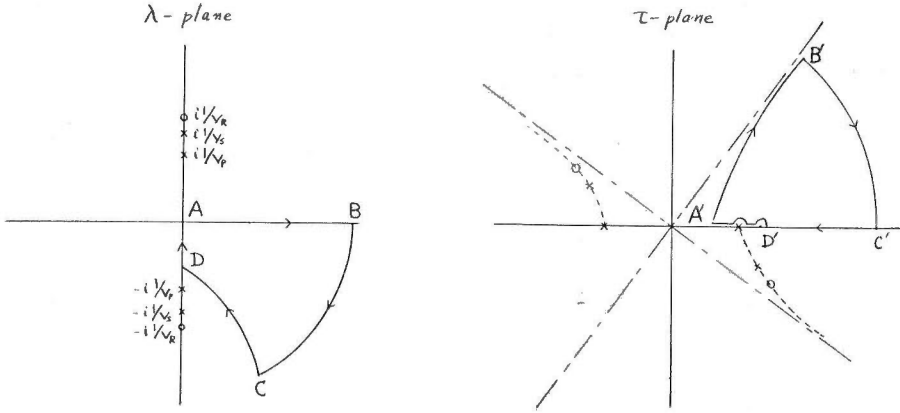

λ - plane τ - plane

Fig. 5

Thus we get the final expression for the displacement in the original space,

$$u\,(x,z,t) = -\,I_m\left\{ G_0\,(\lambda)\frac{\partial\lambda}{\partial\tau_1}\bigg|_{t=\tau_1} - G_0\,(\lambda)\frac{\partial\lambda}{\partial\tau_2}\bigg|_{t=\tau_2} - G_1\,(\lambda)\frac{\partial\lambda}{\partial\tau_2}\bigg|_{t=\tau_2} + G_2\,(\lambda)\frac{\partial\lambda}{\partial\tau_3}\bigg|_{t=\tau_3}\right\}$$

$$w\,(x,z,t) = R_e\left\{ \frac{\partial\lambda}{\partial\tau_1}\bigg|_{t=\tau_1} + \frac{\partial\lambda}{\partial\tau_2}\bigg|_{t=\tau_2} + G_3\,(\lambda)\frac{\partial\lambda}{\partial\tau_2}\bigg|_{r=\tau_3} - G_4\,(\lambda)\frac{\partial\lambda}{\partial\tau_3}\bigg|_{t=\tau_3}\right\}$$

$$\tau_1 > \frac{\sqrt{x^2 + (f-z)^2}}{V_p}, \ \ \tau_2 > \frac{\sqrt{x^2+(f+z)^2}}{V_p}, \ \ \tau_3 > \tau_{30}. \qquad (2.33)$$

where

$$\left\{ \begin{aligned} &\frac{\partial\lambda}{\partial\tau_{1,2}} = \frac{1}{x^2+(f\mp z)^2}\left\{ -ix + \frac{\tau_{1,2}{}^2}{\sqrt{\tau_{1,2}{}^2 - \dfrac{x^2+(f\mp z)^2}{V_p{}^2}}}\right\} \\[2mm] &\lambda = \frac{1}{x^2+(f\mp z)^2}\left\{ -ix\,\tau_{1,2} + (f\mp z)\sqrt{\tau_{1,2}{}^2 - \frac{x^2+(f\mp z)^2}{V_p{}^2}}\right\} \end{aligned}\right.$$

$$\left\{ \begin{aligned} &\frac{\partial\tau_3}{\partial\lambda} = \frac{f\lambda}{\sqrt{\lambda^2 + \dfrac{1}{V_p{}^2}}} + \frac{zf}{\sqrt{\lambda^2 + \dfrac{1}{V_s{}^2}}} + ix \\[2mm] &\tau_3 = \sqrt{\lambda^2 + \frac{1}{V_p{}^2}}\,f + \sqrt{\lambda^2 + \frac{1}{V_s{}^2}}\,z + i\lambda x\ . \end{aligned}\right. \qquad (2.34)$$

Numerical computation for this formula will bring us exact form of transient elastic wave at every point in the medium. However the computation of $\partial\lambda/\partial\tau_3$ is complicated.

The first term of (2.33) is the source wave, and the second term represents the perfect image source reflection. The third term represents the wave which compensates the conversion from dilatational wave to equi-voluminal wave at the surface, and is called a correction term to the perfect image source reflection by Dix[6]. The fourth term is the equi-voluminal wave generated at the surface.

The wave front of this wave has been treated by Cagniard[3]. According to him, the wave front is interpreted as follows. Putting $\lambda = -il$, and

$$l = \frac{\sin \theta_1}{V_p} = \frac{\sin \theta_2}{V_s} \quad ,$$

$\partial \tau_3 / \partial \lambda$ is expressed by θ_1 and θ_2, becoming

$$-\frac{\partial \tau_3}{\partial \lambda} = -i\,(f \tan \theta_1 + z \tan \theta_2 - x) \quad . \tag{2.35}$$

Wave front of the first break is obtained at the time where $\partial \tau_3 / \partial \lambda = 0$. We denoted this time τ_3 as τ_{30}. Then we get

$$\tau_{30} = \frac{R_1}{V_p} + \frac{R_2}{V_s} \tag{2.36}$$

where

$$R_1 = f/\cos \theta_1 \quad , \qquad R_2 = z/\cos \theta_2$$

This minimum time corresponds to the path of Snell's law as is seen in Fig. 6.
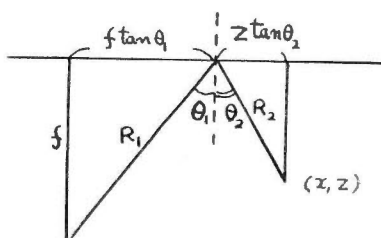
Fig. 6

Wave fronts of u_0, u_{10}, u_{11} and u_2 are illustrated in Fig. 7.
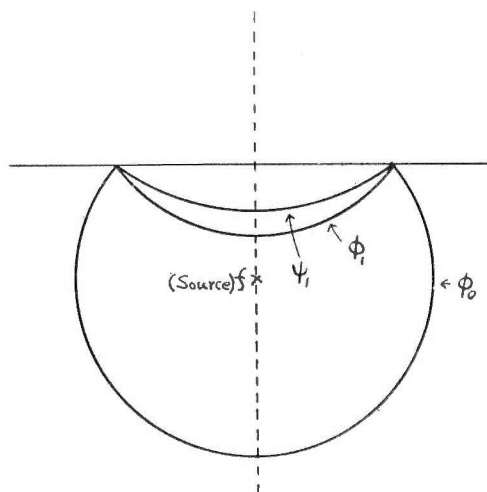
Fig. 7 Wav front of each term

The solution at the surface becomes slightly simple form. Because τ_1, τ_2 and τ_3 become the same each other as is seen from (2.31),

$$\tau_1 = \tau_2 = \tau_3 = \sqrt{\lambda^2 + \frac{1}{V_p{}^2}} \, f + i\lambda x \tag{2.37}$$

and

$$
\begin{aligned}
\frac{\partial \lambda}{\partial \tau} &= \frac{1}{f^2 + x^2} \left\{ - ix + \frac{f\tau}{\sqrt{\tau^2 - \dfrac{f^2 + x^2}{V_p{}^2}}} \right\} \\
&= \frac{1}{f(1 + \xi^2)} \left\{ - i\xi + \frac{\tau'}{\sqrt{\tau'^2 - 1}} \right\}
\end{aligned}
\tag{2.38}
$$

where

$$
\begin{cases}
\tau' = \tau / \sqrt{f^2 + x^2} / V_p \\
\xi = x/f
\end{cases}
\tag{2.39}
$$

and

$$
\begin{cases}
\lambda = \dfrac{1}{f^2 + x^2} \left\{ - ix\tau + f\sqrt{\tau^2 + \dfrac{x^2 + f^2}{V_p{}^2}} \right\} \\
\;\;= \dfrac{1}{V_p \sqrt{1 + \xi^2}} \left\{ - i\xi\tau' + \sqrt{\tau'^2 - 1} \right\}
\end{cases}
\tag{2.40}
$$

The first term and the second term of the horizontal displacement are cancelled out. However the first and the second term of the vertical displacement are additive. Thus we get from (2.33),

$$
\begin{cases}
u(x, o, t) = I_m \left[\left\{ G_1(\lambda) - G_2(\lambda) \right\} \dfrac{\partial \lambda}{\partial \tau} \bigg|_{t=\tau} \right] \\
w(x, o, t) = R_e \left[\left\{ 2 + G_3(\lambda) - G_4(\lambda) \right\} \dfrac{\partial \lambda}{\partial \tau} \bigg|_{t=\tau} \right]
\end{cases}
\tag{2.41}
$$

These formula (2.41) (2.40) (2.39) are the same ones obtained by Garvin[8], who presented numerical examples of these results and explained the generation of Rayleigh wave and surface-S wave.

II. 4 Remarks on other methods

The differences of the method developed in this paper to other methods were briefly mentioned in I.7, Chapter I. The so-called method of integral representation of the solution, used by many investigators since Lamb, will correspond to the inverse transformation of the method of integral transformation. The integration with respect to ζ in Lapwood's paper[18] will correspond to the inverse Fourier transformation, and the integration with respect to ω will correspond to the inverse Laplace transformation in this paper.

A simple mathematical formulation obtained in this paper is a result of treating quantities in the transformed space, where integral representation is no longer required. The greater difference of this method to the method of integral representation will be the use of proper source function and the proper path of

integration, which lead the solution to the exact solution. Both Cagniard's method and this method select a suitable path of integration in the transformed plane, τ-plane, so that exact solution is obtained. While other methods stuck to the λ-plane, and are forced to make approximate evaluation using pole integral and branch line integral with steepest decent method or stationary phase method (cf : Honda and Nakamura[10]). However, there is a path in the λ-plane which leads the solution to an exact form, when the source function is properly selected, as shown in Fig. 2, Chapter I and Fig. 5, Chapter II. This path does not come close to Rayleigh pole and the branch points except special case of solution at the surface. Since the path of integration is a little off these singular points, the contributions from them will not appear as separated terms. They result in an amplitude variation with time. The amount of contributions from pole and branch points will be estimated by the distance between the path and the singular points and the " topography " of the integrand in the λ-plane. Dix[7] has attempted to figure out this situation.

Takeuchi and Kobayashi[26] have replaced exponential term in the integral representation by δ-function. This may correspond to the whole process of Laplace transformation, selection of source function and the inverse Laplace transformation. However, there is some uncertainty concerning the form of the source function used.

The difference between Cagniard's method and this method is not essential. They are equivalent. The only difference is that the mathematical technique developed by Cagniard is naturally introduced. However, when his method is understood as the method of dual integral transformation, this will open another field of application. An example will be seen in Chapter IV, for diffraction problem.

III. Reflection and Refraction of an Acoustic Pressure Pulse at a Liquid-liquid Interface

III. 1 Introduction

Let us apply the method of integral transformation to reflection and refraction phenomena. Cagniard[3] has made extensive and rigorous treatment for reflection and refraction of transient elastic wave at the solid-solid interface in the three dimensional case. His results, wave fronts of many waves, which are deduced from exact solutions, have given many lights on the mechanism of reflection and refraction of a transient pulse which has a curved wave front. By using his method, Spencer[23] has studied the mechanism of reflection at the liquid-solid interface under the source point. However, wave forms of reflected and refracted waves have not yet obtained due to difficulties of three-dimensional treatment.

On the other hand, Honda and Nakamura[11] and Takeuchi and Kobayashi[27] have studied this problem for the SH-pulse and have presented wave forms. However, because of their method used, mechanism of reflection and refraction is not fully elucidated.

In order to clear up the basic picture of reflection and refraction phenomena of a transient wave with a curved wave front, the case of liquid-liquid interface is taken and studied in two dimensions in this chapter.

Wave forms of reflection and refraction, which are numerically computed from exact solutions obtained in III. 3, are illustrated in III. 4. And variation of reflection coefficient with angle of incidence is also illustrated in III. 4. Mechanism of reflection and refraction is described in detail in III. 4.

III. 2 Formal solutions

Let us consider the system of liquid-liquid interface shown in Fig. 8. The x-y axes are taken on the interface and the z-axis is directed vertically upward. The density, velocity of acoustic wave and displacement potential are denoted by ρ, V and ϕ respectively. The suffixes 1 and 2 refer to the upper medium and the lower one respectively.
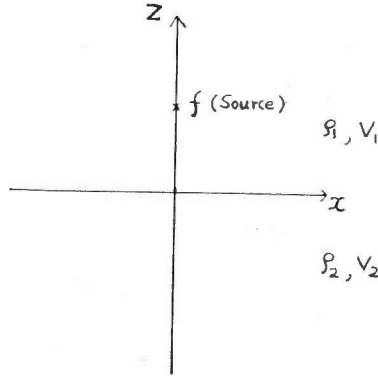
Fig. 8

The line source is located in the upper medium at $z = f$, $x = 0$. Then, Laplace-Fourier transformed wave equations are

$$\begin{cases} \dfrac{d^2\bar{\phi}_1}{dz^2} - (\xi^2 + h_1{}^2)\, \bar{\phi}_1 = 0 \\[2mm] \dfrac{d^2\bar{\phi}_2}{dz^2} - (\xi^2 + h_2{}^2)\, \bar{\phi}_2 = 0 \end{cases} \tag{3.1}$$

where

$$h_1{}^2 = p^2/V_1{}^2 \quad , \qquad h_2{}^2 = p^2/V_2{}^2 \quad . \tag{3.2}$$

The Laplace-Fourier transformed boundary conditions to be satisfied at the interface $z = 0$ are, according to continuities of stress and displacement,

$$\begin{cases} \rho_1\bar{\phi}_1 = \rho_2\bar{\phi}_2 \\[2mm] \dfrac{\partial\bar{\phi}_1}{\partial z} = \dfrac{\partial\bar{\phi}_2}{\partial z} \end{cases} . \tag{3.3}$$

When the displacement potential of the source function is taken as

$$\bar{\phi}_0\,(\xi,\, z,\, p) = A_0\; e^{\mp\sqrt{\xi^2+h_1{}^2}\,(f-z)} \qquad \text{for } z \lessgtr f \tag{3.4}$$

in the Laplace-Fourier transformed space, general solutions of wave equation

24

(3.1) become

$$
\begin{cases}
\bar{\phi}_1(\bar{\xi}, z, p) = \bar{\phi}_0 + A\ e^{-\sqrt{\xi^2+h_1^2}\ z} \\
\bar{\phi}_2(\bar{\xi}, z, p) = \qquad B\ e^{+\sqrt{\xi^2+h_2^2}\ z}
\end{cases}
\tag{3.5}
$$

Coefficients A and B are determined by putting (3.5) into (3.3),

$$
\begin{cases}
A = -A_0\ e^{-\sqrt{\xi^2+h_1^2}\ f} + \dfrac{2\rho_2\sqrt{\xi^2+h_1^2}}{\rho_1\sqrt{\xi^2+h_2^2}+\rho_2\sqrt{\xi^2+h_1^2}}\ A_0\ e^{-\sqrt{\xi^2+h_1^2}\ f} \\[3mm]
B = \qquad\qquad \dfrac{2\rho_1\sqrt{\xi^2+h_1^2}}{\rho_1\sqrt{\xi^2+h_2^2}+\rho_2\sqrt{\xi^2+h_1^2}}\ A_0\ e^{+\sqrt{\xi^2+h_1^2}\ f}
\end{cases}
\tag{3.6}
$$

Thus, the displacement potentials in the transformed space become

$$
\begin{cases}
\bar{\phi}_1 = \bar{\phi}_0 + \bar{\phi}_{10} + \bar{\phi}_{11} \\
\bar{\phi}_2 = \bar{\phi}_2
\end{cases}
\tag{3.7}
$$

where

$$
\bar{\phi}_{10} = -A_0\ e^{-\sqrt{\xi^2+h_1^2}\ (f+z)}
$$

$$
\begin{cases}
\bar{\phi}_{11} = \dfrac{2\rho_2\sqrt{\xi^2+h_1^2}}{\rho_1\sqrt{\xi^2+h_2^2}+\rho_2\sqrt{\xi^2+h_1^2}}\ A_0\ e^{-\sqrt{\xi^2+h_1^2}\ (f+z)} \\[3mm]
\bar{\phi}_2 = \dfrac{2\rho_1\sqrt{\xi^2+h_1^2}}{\rho_1\sqrt{\xi^2+h_2^2}+\rho_2\sqrt{\xi^2+h_1^2}}\ A_0\ e^{-\sqrt{\xi^2+h_1^2}\ f}\ e^{+\sqrt{\xi^2+h_2^2}\ z}
\end{cases}
\tag{3.8}
$$

$\bar{\phi}_{10}$ represents the wave from the perfect image source. $\bar{\phi}_{11}$ represents the wave which compensates the perfect image source reflection for the energy transmission into the lower medium, and is called correction term by Dix[6]. $\bar{\phi}_2$ represents the transmitted wave into the lower medium.

The differential pressure associated with acoustic wave is expressed by

$$
dp = -\rho\ \frac{\partial^2}{\partial t^2}\ \phi \qquad\qquad *
\tag{3.9}
$$

because ϕ is the displacement potential. Therefore, the formal solutions of the differential pressure in the original space (x, z, t) are given by

* From the definition of differential pressure dp,

$$
dp = -k\ \Theta = -k\ \nabla^2\phi = -k\ \frac{1}{V^2}\ \frac{\partial^2\phi}{\partial t^2} = -\rho\ \frac{\partial^2\phi}{\partial t^2}
$$

where k: bulk modulus, Θ: dilatation.

One may regard ϕ_0 as a velocity potential and take a differential pressure by the relation of $dp = -\rho\ \dfrac{\partial\phi_0}{\partial t}$. The reason why ϕ_0 is not taken as a velocity potential is that the differential pressure associated with the source function $\phi_0 = \cosh^{-1}\ t/r/V$ is not physical. Because the particle velocity given by this velocity potential approaches to $1/r$ with time, meaning constant particle velocity.

$$\begin{cases} dp_1 = -\rho_1 \dfrac{\partial^2}{\partial t^2} L^{-1} \cdot F^{-1} [\bar{\phi}_1] \\[2mm] dp_2 = -\rho_2 \dfrac{\partial^2}{\partial t^2} L^{-1} \cdot F^{-1} [\bar{\phi}_2] \ . \end{cases} \tag{3.10}$$

where L^{-1}, F^{-1} denote the operation of inverse transformation;

$$\begin{cases} L^{-1} \equiv \dfrac{1}{2\pi i} \displaystyle\int_{c-i\infty}^{c+i\infty} e^{pt}\, dp, \\[3mm] F^{-1} \equiv \dfrac{1}{\sqrt{2\pi}} \displaystyle\int_{-\infty}^{\infty} e^{-i\xi x}\, d\xi \ . \end{cases} \tag{3.11}$$

III. 3 Evaluation of the inverse transformation

First, we introduce the same source function as is used in the preceding chapters;

$$\phi_0 = \begin{cases} 0 \\ \cosh^{-1} t/r/V_1 \end{cases} \qquad \text{for} \qquad \begin{array}{l} t < r/V_1 \\ t > r/V_1 \end{array} \tag{3.12}$$

$$r = \sqrt{x^2 + (f-z)^2} \ ,$$

and $\tag{3.13}$

$$A_0 = \sqrt{\frac{\pi}{2}} \cdot \frac{1}{p} \cdot \frac{1}{\sqrt{\xi^2 + h_1^2}} \ .$$

Then we convert the parameter ξ to λp, $\xi = \lambda p$. In order to lead the integration of (3.10) to a closed form, the inverse transformation is applied to $\rho \dfrac{\partial \phi}{\partial t}$, and differential pressure solution is obtained from $\rho \dfrac{\partial \phi}{\partial t}$ by the numerical differentiation.

The evaluation of ϕ_{10}, the perfect image source reflection, is directly obtained and becomes

$$\phi_{10} = \begin{cases} 0 \\ \cosh^{-1} t/r'/V_1 \end{cases} \qquad \text{for} \qquad \begin{array}{l} t < r'/V_1 \\ t > r'/V_1 \end{array} \tag{3.14}$$

$$r' = \sqrt{x^2 + (f+z)^2}$$

because $\bar{\phi}_{10}$ has the same form with the source function.

The evaluations of ϕ_{11} and ϕ_2 are made as follows. From (3.10) (3.11) and (3.13), we get

$$\rho_1 \frac{\partial \phi_{11}}{\partial t} = L^{-1} \cdot \frac{1}{2} \int_{-\infty}^{\infty} G(\lambda) \exp(-p\tau_1)\, d\lambda \tag{3.15}$$

$$\rho_2 \frac{\partial \phi_2}{\partial t} = L^{-1} \cdot \frac{1}{2} \int_{-\infty}^{\infty} G(\lambda) \exp(-p\tau_2)\, d\lambda \tag{3.16}$$

where

$$G(\lambda) = \frac{2\rho_1 \rho_2}{\rho_1 \sqrt{\lambda^2 + \dfrac{1}{V_2^2}} + \rho_2 \sqrt{\lambda^2 + \dfrac{1}{V_1^2}}} \tag{3.17}$$

$$\begin{cases} \tau_1 = \sqrt{\lambda^2 + \dfrac{1}{V_1{}^2}} \, (f + z) + i\lambda x \\ \tau_2 = \sqrt{\lambda^2 + \dfrac{1}{V_2{}^2}} \, f - \sqrt{\lambda^2 + \dfrac{1}{V_2{}^2}} \, z + i\lambda x \quad . \end{cases} \tag{3.18}$$

Since the integrand $G(\lambda)$ and a part of exponential term are the even functions of λ, and since

$$e^{-i\lambda px} = \cos \lambda px - i \sin \lambda px$$

the domain of integration of λ is changed into from 0 to infinity;

$$\begin{cases} \rho_1 \dfrac{\partial \phi_{11}}{\partial t} = L^{-1} \cdot R_e \displaystyle\int_0^\infty G(\lambda) \, \exp(-p\tau_1) \, d\lambda \\ \rho_2 \dfrac{\partial \phi_2}{\partial t} = L^{-1} \cdot R_e \displaystyle\int_0^\infty G(\lambda) \, \exp(-p\tau_2) \, d\lambda \quad . \end{cases} \tag{3.19}$$

Then, changing the order of integration of Laplace inversion and Fourier inversion, we have

$$\begin{cases} \rho_1 \dfrac{\partial \phi_{11}}{\partial t} = R_e \displaystyle\int_0^\infty G(\lambda) \, \delta(t - \tau_1) \, d\lambda \\ \rho_2 \dfrac{\partial \phi_2}{\partial t} = R_e \displaystyle\int_0^\infty G(\lambda) \, \delta(t - \tau_2) \, d\lambda \quad . \end{cases} \tag{3.20}$$

Because of δ-function, involving τ as a function of λ, we change the integration parameter λ to τ. Thus we get

$$\begin{cases} \rho_1 \dfrac{\partial \phi_{11}}{\partial t} = R_e \displaystyle\int_{L_1} G(\lambda) \, \delta(t - \tau_1) \, \dfrac{\partial \lambda}{\partial \tau_1} \, d\tau_1 \\ \rho_2 \dfrac{\partial \phi_2}{\partial t} = R_e \displaystyle\int_{L_2} G(\lambda) \, \delta(t - \tau_2) \, \dfrac{\partial \lambda}{\partial \tau_2} \, d\tau_2 \quad , \end{cases} \tag{3.21}$$

where L_1 and L_2 are the integration path on the τ-plane corresponding to the path on the λ-plane. And λ and $\partial \lambda / \partial \tau_1$ are given from (3.18) by

$$\begin{cases} \lambda = \dfrac{1}{x^2 + (f + z)^2} \left\{ -ix\tau + (f + z) \sqrt{\tau_1{}^2 - \dfrac{x^2 + (f + z)^2}{V_1{}^2}} \right\} \\ \dfrac{\partial \lambda}{\partial \tau_1} = \dfrac{1}{x^2 + (f + z)^2} \left\{ -ix + \dfrac{(f + z)\tau_1}{\sqrt{\tau_1{}^2 - \dfrac{x^2 + (f + z)^2}{V_1}}} \right\} \end{cases} \tag{3.22}$$

The expression of $\partial \lambda / \partial \tau_2$ as a function of τ_2 is very complicated.

Let us see the path of integration on both λ-plane and τ_1-plane. The transformation of λ-plane to τ_1-plane is done in the similar way as described in the preceding chapters. Here we take the case $V_2 > V_1$. Referring to Fig. 9, the positive axis of λ-plane is transformed to the line A′ B′ in the τ_1-plane. The imaginary axis of λ-plane is transformed to the dotted line in the τ_1-plane. This dotted line folds back at the point $\tau_1 = \sqrt{(f + z)^2 + x^2}/V_1$, D′, where $\partial \tau_1 / \partial \lambda = 0$.
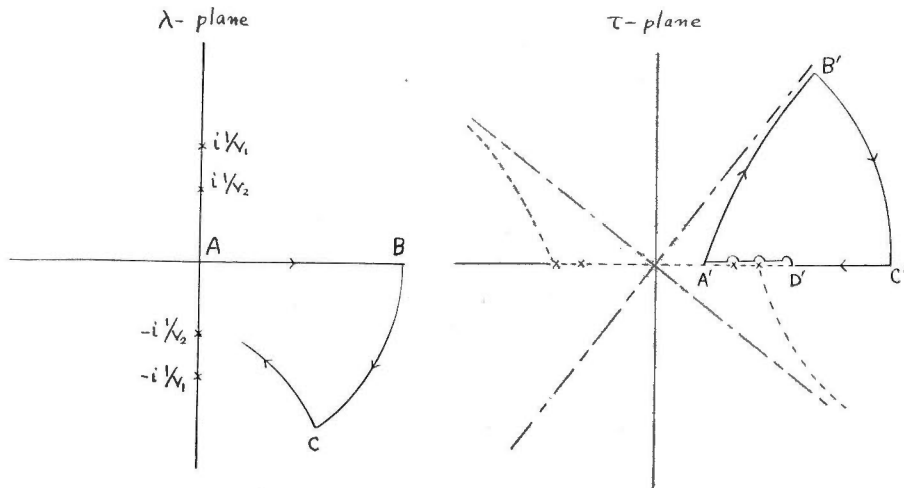
λ- plane   τ- plane

Fig. 9

This point is the pole of $\partial\lambda/\partial\tau_1$. Branch points on the imaginary axis of λ-plane, $\lambda = \pm i\dfrac{1}{V_1}$ and $\lambda = \pm i\dfrac{1}{V_2}$, are transformed on the real axis of τ_1-plane at $\tau = \mp x/V_1$ and $\tau = \mp\dfrac{x}{V_2} + \sqrt{-\dfrac{1}{V_1{}^2} - \dfrac{1}{V_2{}^2}}\,(f+z)$. In order to evaluate the integration of (3.21), we add, on the τ_1-plane, path B′ C′ at a great distance, and path C′ A′ on the real positive axis, avoiding pole and branch points with small indentation on the upper side. These paths form a closed path within which there are neither pole nor branch points. Then we get from Cauchy's theorem

$$\int_{A'B'} = -\int_{B'C'} - \int_{C'A'} \quad .$$

The integration on the path B′ C′ vanishes, because of large value of λ and $G(\lambda) \propto 1/\lambda$. Thus, integration required is for the path on the real axis. However, on the real axis of τ_1-plane, there are branch points and a pole. Let us see in detail the configuration of the path on the λ-plane.
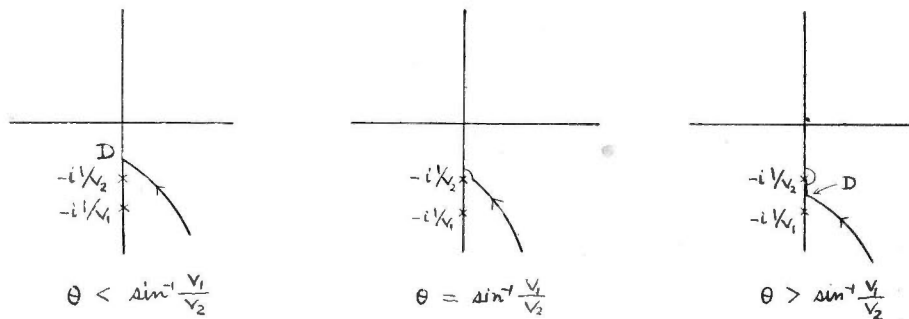
Fig. 10

The path B′ C′ in the τ_1-plane corresponds to the path BC in the λ-plane. The transformation of the path C′ A′ in the τ_1-plane to the path CA in the λ-plane depends upon the case, and is shown in Fig. 10. This transformation is obtained as follows. From (3.22), it is seen that λ becomes purely imaginary when $\tau_1 < \sqrt{x^2 + (f+z)^2}/V_1$. Let us denote this point D and D′ on the λ-plane and τ_1-plane respectively. Thus the path D′A′ on the real axis of τ_1-plane corresponds to the path DA, a portion of imaginary axis of λ-plane. The path CD is on the complex-plane of λ. The value of λ at the point D is

$$\lambda = -i \frac{x}{(f+z)^2 + x^2} \cdot \frac{1}{V_1} \quad,$$

and is rewritten by

$$\lambda = -i \frac{\sin\theta}{V_1}$$

where θ is the angle shown in Fig. 11.
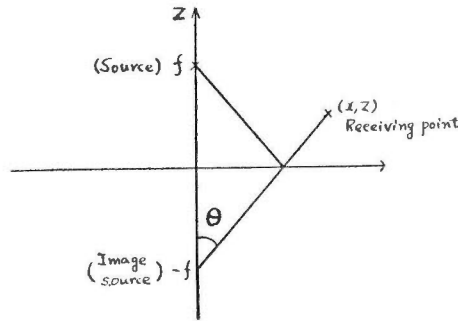
Fig. 11

Therefore, the location of the point D on the imaginary axis is above, at or below of the branch point, $-i\frac{1}{V_2}$, according to the condition $\theta \lessgtr \sin^{-1} V_1/V_2$. The point D is always above the other branch point, $-i\frac{1}{V_1}$.

Now, let us evaluate the integration on the path CDA on the λ-plane.

(i) The case of $\theta < \sin^{-1} V_1/V_2$

The integral on the path DA vanishes, because of purely imaginary value of $G(\lambda)\frac{\partial\lambda}{\partial\tau_1}$. Therefore, the contribution to the results is made only from the path C′D′, becoming

$$Re\int_{C'D'} = Re\left\{ G(\lambda) \frac{\partial\lambda}{\partial\tau_1}\Big|_{t=\tau_1} \right\} \qquad \tau > \frac{\sqrt{x^2 + (f+z)^2}}{V_1} \qquad (3.23)$$

(ii) The case of $\theta > \sin^{-1} V_1/V_2$

On the path DA, the contribution from the segment of path $\lambda < -i\frac{1}{V_2}$ vanishes. However there is a contribution from a segment of path $-i\frac{1}{V_2} < \lambda < -i\frac{\sin\theta}{V_1}$,

because of complex value of $G(\lambda)$ in this interval. Therefore the contribution to the results is made from this segment and C′D′, becoming,

$$R_e \left\{ G(\lambda) \frac{\partial \lambda}{\partial \tau_1} \bigg|_{t=\tau_1} \right\} \qquad \tau_1 > \frac{x}{V_2} + \sqrt{\frac{1}{V_1{}^2} - \frac{1}{V_2{}^2}} \, (f+z) \quad . \qquad (3.24)$$

Thus, the final expression is given by

$$\rho_1 \frac{\partial \phi_1}{\partial t} = \rho_1 \left\{ \frac{\partial \phi_0}{\partial t} + \frac{\partial \phi_{10}}{\partial t} + \frac{\partial \phi_{11}}{\partial t} \right\} \qquad\qquad (3.25)$$

and

$$\rho_1 \frac{\partial \phi_{11}}{\partial t} = R_e \left\{ G(\lambda) \frac{\partial \lambda}{\partial \tau} \bigg|_{t=\tau_1} \right\} \qquad\qquad (3.26)$$

$$\tau_1 > \frac{x}{V_1} + \sqrt{\frac{1}{V_1{}^2} - \frac{1}{V_2{}^2}} \, (f+z) \quad \text{for} \quad \theta > \sin^{-1} V_1/V_2$$

$$\tau_1 > \frac{\sqrt{x^2 + (f+z)^2}}{V_1} \qquad\qquad \text{for} \quad \theta < \sin^{-1} V_1/V_2$$

where $G(\lambda)$ and $\partial \lambda/\partial \tau_1$, are given in (3.17) and (3.22); ϕ_0 and ϕ_{10} are given in (3.12) and (3.14) respectively.

So far we have investigated the case $V_2 > V_1$. However, the case $V_2 < V_1$ is more easily treated, because the branch point of V_2 does not lie on the real axis of τ-plane. The results are the same as that obtained in (3.25) (3.26) except the value of τ_1. The time of the first break, τ_1, is always $\sqrt{x^2 + (f+z)^2}/V_1$ for any value of θ.

III. 4 Interpretation and numerical results

(i) Wave front

The wave front of the first break of reflected and refracted waves is obtained from the smallest value of time τ_1 in (3.26). When a receiving point is located within the critical angle, i.e. $\theta < \sin^{-1} V_1/V_2$ as shown in Fig. 12, the wave fronts of perfect image reflection ϕ_{10} and compensation ϕ_{11} arrive at the same time, $\tau_1 = \dfrac{\sqrt{x^2 + (f+z)^2}}{V_1}$. When a receiving point is located outside of the critical angle, i.e. $\theta > \sin^{-1} V_1/V_2$, the wave front of the compensation arrives as the first break at the time $\tau_1 = \dfrac{x}{V_2} + \sqrt{\dfrac{1}{V_1{}^2} - \dfrac{1}{V_2{}^2}} \, (f+z)$, and the wave front of the perfect image reflection arrives later at the time $\tau_1 = \sqrt{x^2 + (f+z)^2}/V_1$. These wave fronts are illustrated in Fig. 12. As is seen on this figure, the wave front of the compensation is a plane, intersecting the interface with the wave front of the refracted wave in the lower medium and contacting the perfect image source reflection wave front at $\theta = \theta_c$. This is the wave front called as the "Conical wave front" by Cagniard[3] in the 3-dimensional case. The arrival time of the conical wave front is equal to that of minimum time path of geometrical optics.

We have seen that the conical wave is derived from the compensation term ϕ_{11}, compensation for the energy transmission into the lower medium.
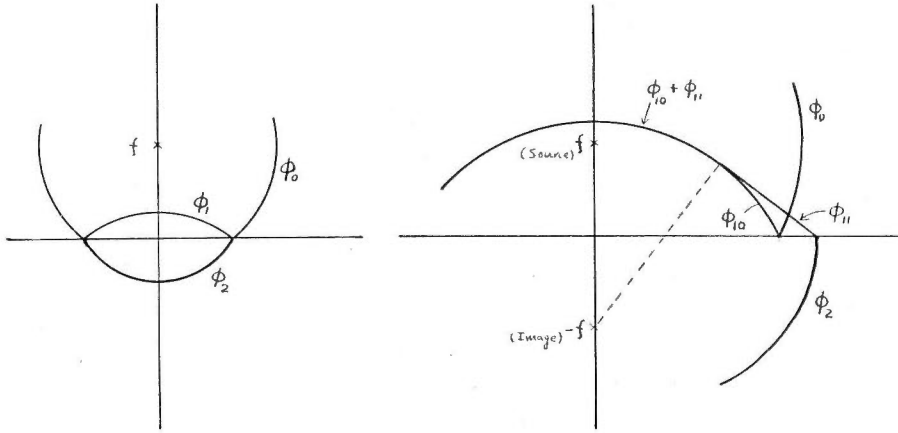
Fig. 12   Wave front of each term

Therefore, it will be naturally understood that the conical wave is always accompanied with the refracted wave in the lower medium and it should form a wave front ahead of the reflection wave front, when the refracted wave in the lower medium proceeds the direct wave front along the interface. From this wave front view-point, the development of conical wave front will be understood as a part of the first break wave front associated with the refracted wave in the lower medium. Therefore, we can expect enough energy for the conical wave. Let us see the exact wave forms in the next paragraph.

(ii)   Wave forms of reflected and refracted waves

For the numerical computation, the expressions of $\rho_1 \dfrac{\partial \phi_{10}}{\partial t}$ and $\rho_1 \dfrac{\partial \phi_{11}}{\partial t}$, (3.26), are rewritten in the form of

$$\rho_1 \frac{\partial \phi_{10}}{\partial t} = \frac{\rho_1}{\tau_0} \frac{1}{\sqrt{\tau_1'^2 - 1}} \qquad \text{for} \quad \tau_1' > 1 \qquad (3.27)$$

$$\rho_1 \frac{\partial \phi_{11}}{\partial t} = R_e \left[\frac{\rho_1}{\tau_0} \frac{2}{\{\sqrt{A} + \dfrac{\rho_1}{\rho_2} \sqrt{B}\}} \left\{ -i \tan \theta + \frac{\tau_1'}{\sqrt{\tau_1'^2 - 1}} \right\} \right] \quad (3.28)$$

$$\text{for} \quad \tau_1' > 1 \ , \quad \theta < \theta_c$$
$$\tau_1' > \cos(\theta - \theta_c) \ , \quad \theta > \theta_c$$

where

$$\begin{cases} A = (\tau_1'^2 - 1) - \tau_1'^2 \tan^2 \theta + \dfrac{1}{\cos^2 \theta} - i\, 2 \tan \theta\, \tau_1' \sqrt{\tau_1'^2 - 1} \\[2mm] B = (\tau_1'^2 - 1) - \tau_1'^2 \tan^2 \theta + \left(\dfrac{V_1}{V_2}\right)^2 \dfrac{1}{\cos^2 \theta} - i\, 2 \tan \theta\, \tau_1' \sqrt{\tau_1'^2 - 1} \quad (3.29) \\[2mm] \tau_1' = \tau_1/\tau_0, \ \tau_0 = \sqrt{x^2 + (f+z)^2}/V_1 \ . \end{cases}$$

τ_1' is the local time. Numerical computation is made for $\theta = 0°$, $10°$, $20°$, $30°$, $40°$, $50°$, $60°$, $70°$, $80°$, in the case of $\rho_1 = \rho_2$ and $\theta_c = 40°$, $(V_1/V_2 = 0.64279)$. The differential pressure form is obtained by the numerical differentiation.
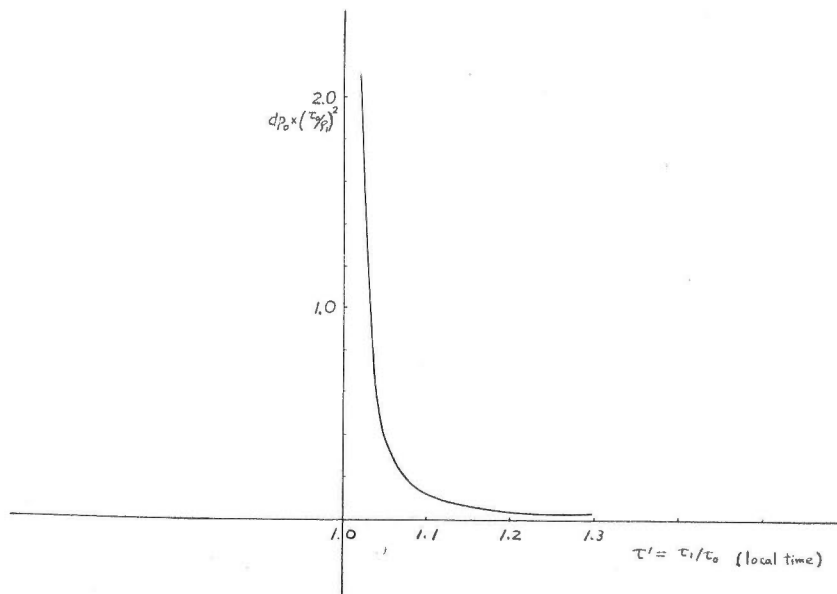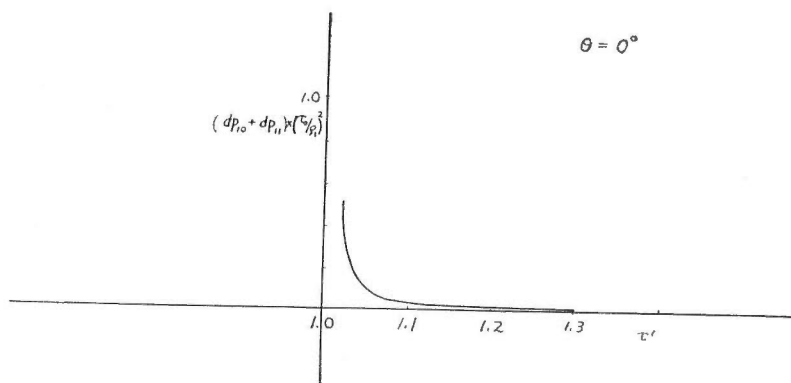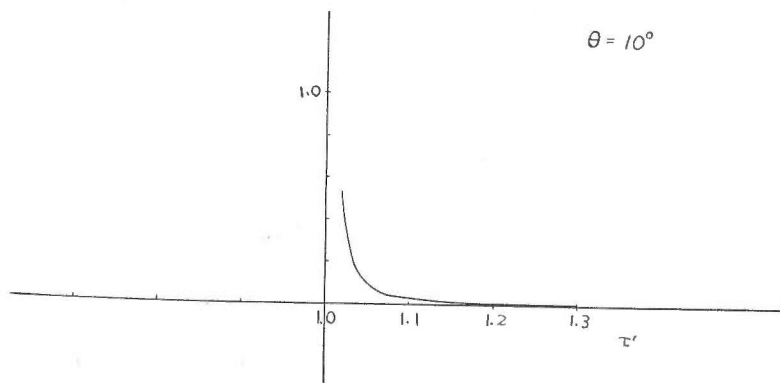
Fig. 13　Pressure form of the source wave

Fig. 14　Pressure form of $\phi_{10} + \phi_{11}$ in the upper medium ; $\theta = 0°$
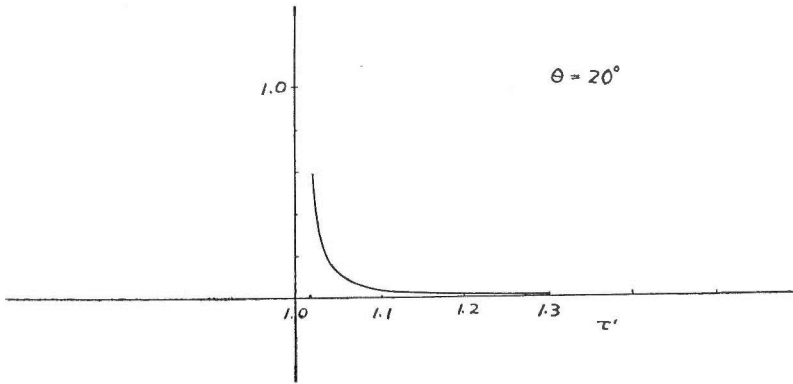

Fig. 15　$\theta = 10°$

Fig. 16 Pressure form of $\phi_{10} + \phi_{11}$ in the upper medium ; $\theta = 20°$
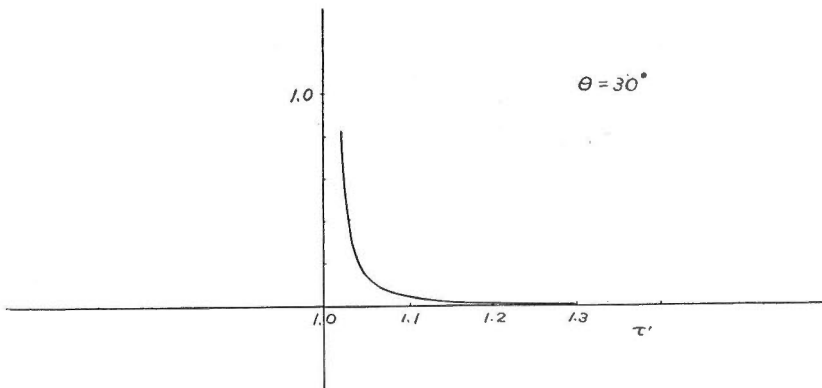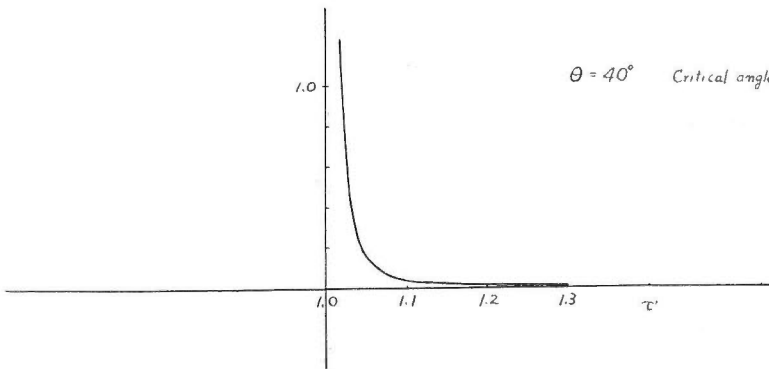

Fig. 17 $\theta = 30°$

Fig. 18 $\theta = 40°$; critical angle

The wave form of the source wave is illustrated in Fig. 13. Reflected and refracted wave forms in the upper medium are illustrated in Figs. 14 ~ 22 according to angle θ (Fig. 11). These figures show the value of $dp \times (\tau_0/\rho_1)^2$, because $(\tau_0/\rho_1)^2$ is the common factor for various receiving points. Refracted
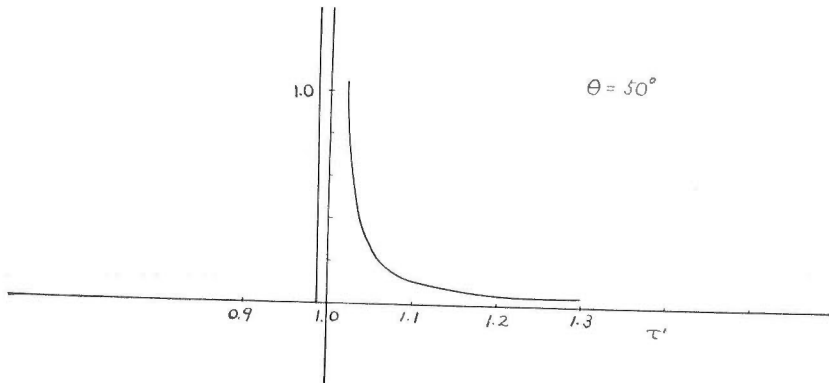
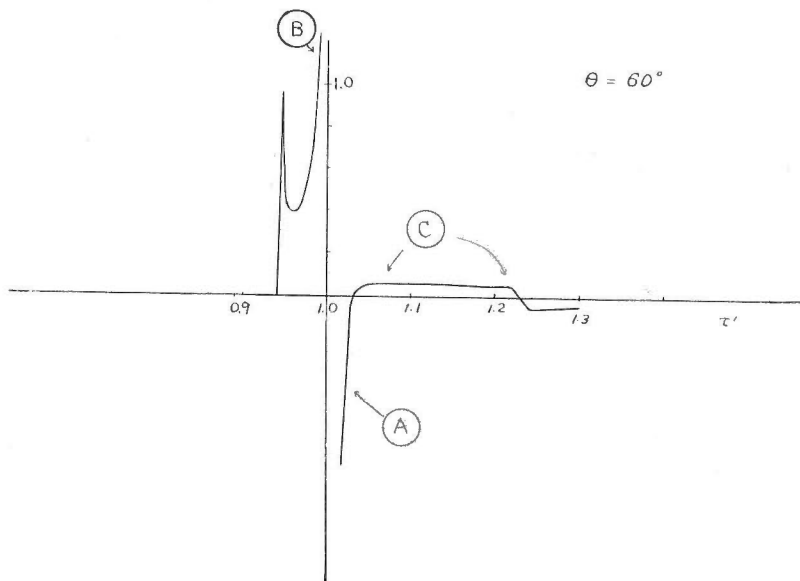Fig. 19 Pressure form of $\phi_{10} + \phi_{11}$ in the upper medium ; $\theta = 50°$

Fig. 20 $\theta = 60°$

wave in the lower medium at the interface is also illustrated in Figs. 23 ~ 27, because ϕ_2 is equal to the compensation term ϕ_{11} at the interface*.

In these figures, we can see several interesting features of reflection and refraction phenomena. The wave form of the refracted wave is a sharp spike with considerable amplitude**. After the first break, the amplitude of disturbance decays with time and then it increases again to the positive infinity as the time

---

* At the interface, it is easily seen from (3.17) and (3.18) that

$$\tau_1 = \tau_2 = \sqrt{\lambda^2 + \frac{1}{V_1{}^2} f + i\lambda x} \quad \text{and} \quad \rho_1\phi_{11} = \rho_2\phi_2$$

** Takeuchi's result[27] on the displacement of SH-pulse differs a little at this point. His result is very similar to $\rho_1 \dfrac{\partial\phi_{11}}{\partial t}$ in this paper. This difference may be due to that of source function.
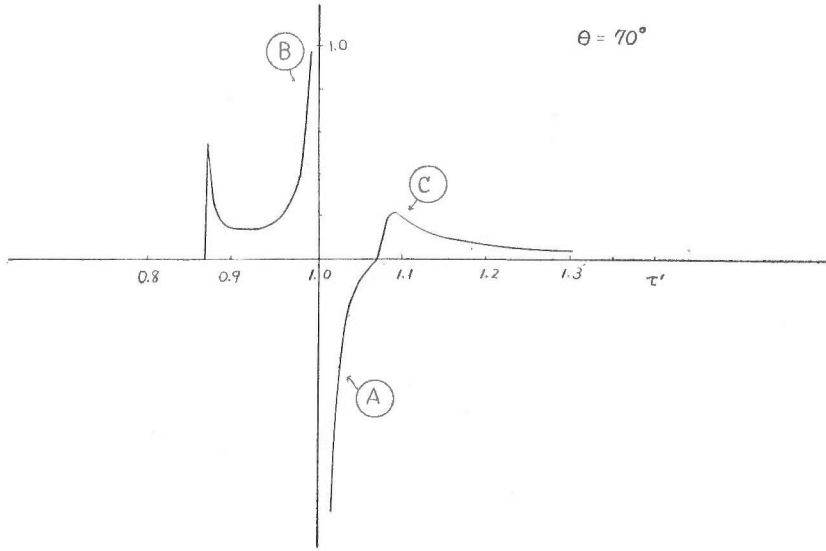
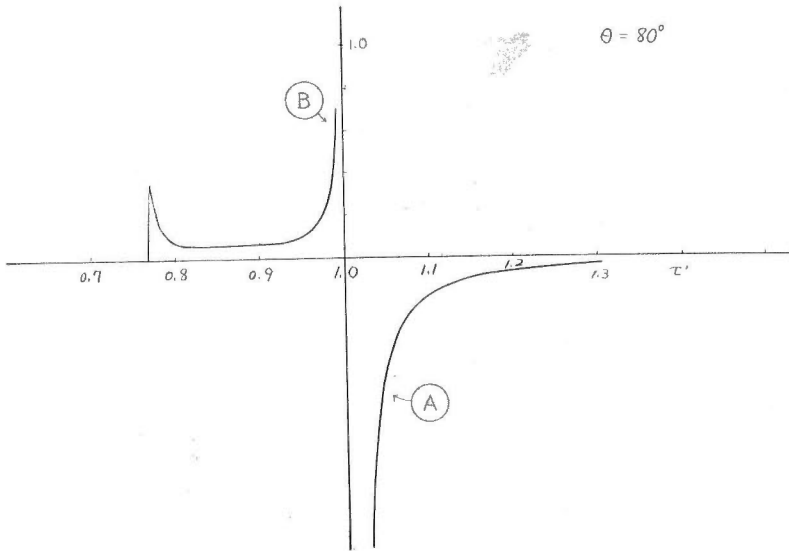Fig. 21   Pressure form of $\phi_{10} + \phi_{11}$ in the upper medium ; $\theta = 70°$

Fig. 22 $\theta = 80°$

approaches to $\tau_1' = 1$. At this time reflected wave front arrives.   The phase of the reflected wave (marked by Ⓐ in figures) is the same as that of direct wave, when receiving point is located within the critical angle.   And, as is well known, the phase inversion takes place when the receiving point is located far beyond the critical angle. The phase inverted reflected wave and the positive phase (marked by Ⓑ in figures) of large amplitude just ahead of the reflected wave form the oscillatory wave form.   Moreover an additional small oscillation
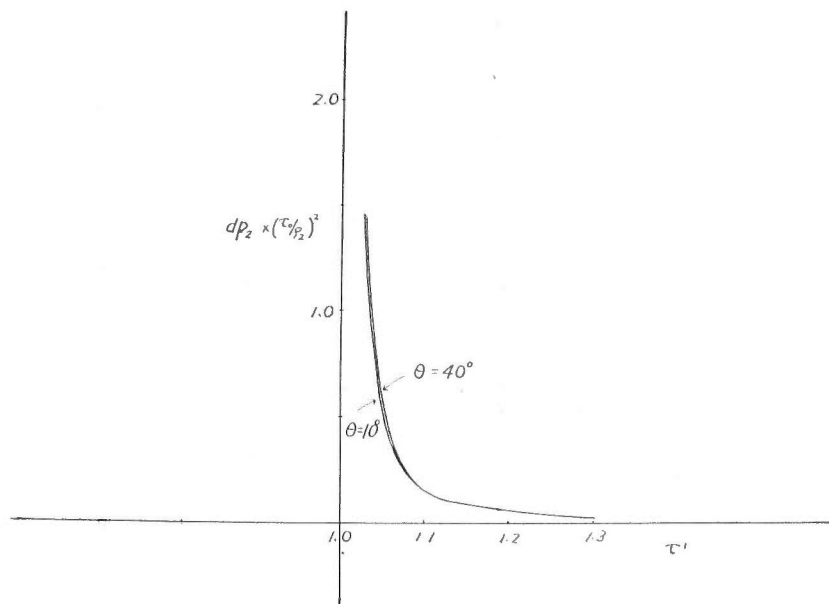
Fig. 23   Pressure form of ϕ_2 at $z = 0$; refracted wave
on the boundary; $\theta = 10 \sim 40°$

(marked by Ⓒ in figures) associated with this phase inversion is seen in the figures 20, 21 at $\theta = 60°$ and $70°$. Thus, the oscillatory feature of the reflection seems to be essential to the reflection beyond the critical angle. Therefore, although it is true that the phase of reflected wave is inversed beyond the critical angle, what is observed as the reflection will be these wave forms, oscillatory wave forms[*].

The refracted wave in the lower medium at the interface also has the sharp spike first break beyond the critical angle. There is another phase of great amplitude (marked by Ⓓ in figures) at the time $\tau_2' = 1$, when the direct wave front arrives at the receiving point on the interface. This shows the transmission of considerable energy from the direct wave into the lower medium at this time[**]. It will be natural to think that there is a considerable energy transmission into the lower medium so far as the direct wave hits the interface even though the point is beyond the critical angle. The energy transmission of this kind may be a cause of boundary wave.

Just ahead of this phase there is another phase of large amplitude, (marked by Ⓔ in figures) which relates to the phase of large amplitude of reflection. These phases will be interpreted as follows. When the cylindrical direct wave front hits the interface, a part of its energy is reflected back and other part is transmitted into the lower medium, forming a reflection and a refraction wave front. The medium behind these wave front is disturbed according to the wave form of source wave. And the energy of these disturbances are supplied

---

[*]   A part of this oscillatory feature is seen in Takeuchi's paper[27].

[**]   The energy transmission of this kind is already reported by Kawasumi[16]. However there is no particular increase of transmitted energy at the critical angle.
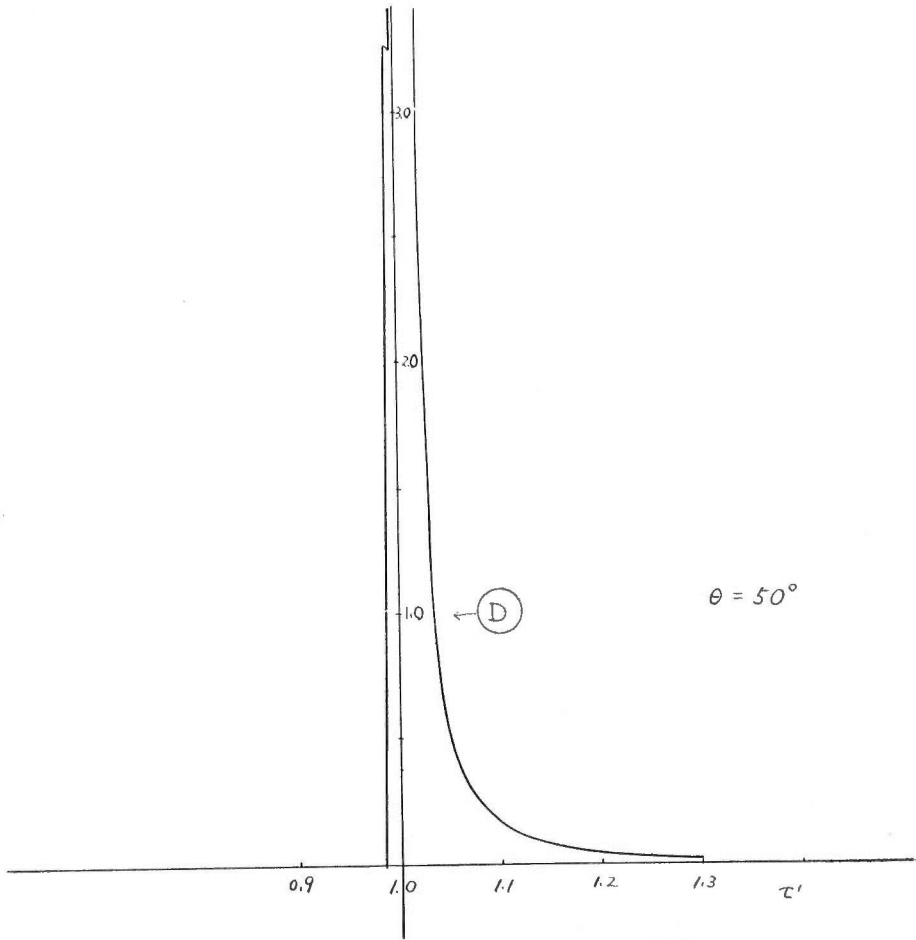
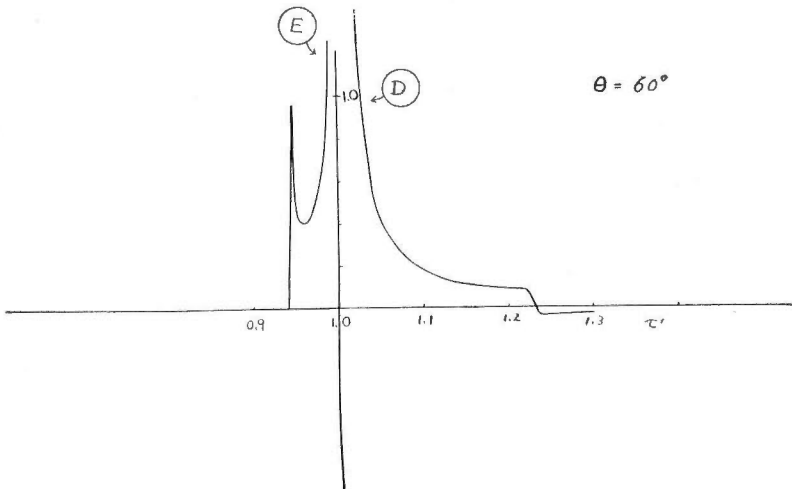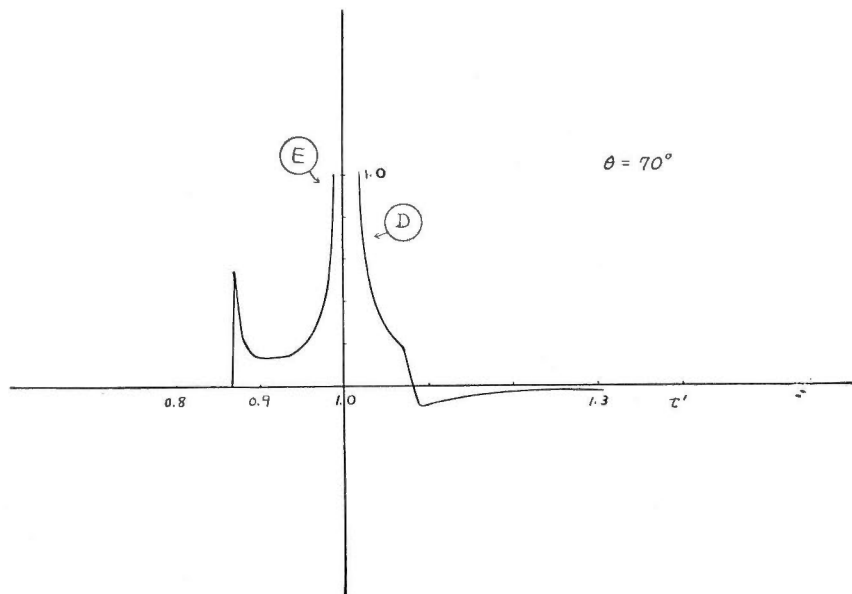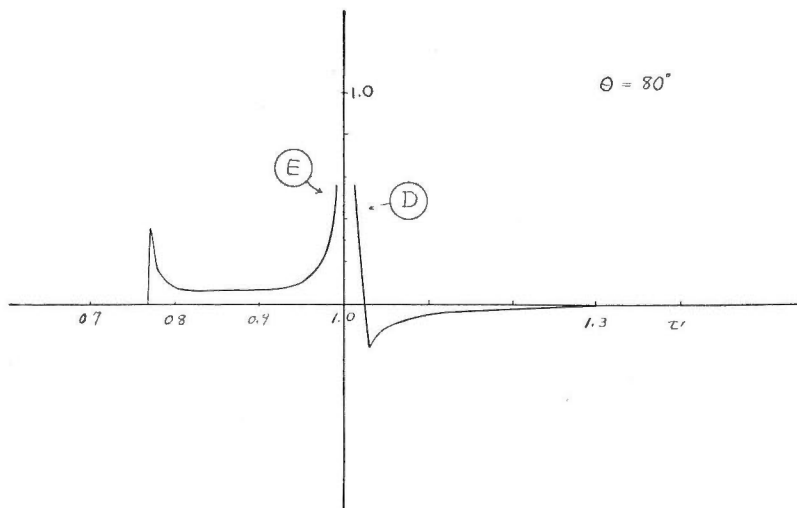Fig. 24   Pressure form of ϕ_2 at $z = 0$; $\theta = 50°$

Fig. 25 $\theta = 60°$

Fig. 26   Pressure form of ϕ_2 at $z = 0$; $\theta = 70°$

Fig. 27 $\theta = 80°$

from every point at the interface which is already hit by the direct wave.   These disturbances in the lower medium propagate with the higher velocity.   And the figures of transmitted wave in the lower medium show the mode of energy accumulation of these disturbances.   Since the wave front of the transmitted wave in the lower medium does not exceed the direct wave front at the interface until it reaches the critical angle, the most of the energy is accumulated at the wave front.   However, because of higher velocity of propagation in the lower medium, the wave front of the transmitted wave gradually exceeds the direct wave front when it goes over the critical angle.   Then a portion of energy,

which has been accumulated at the wave front begins to exceeds the direct wave front. This situation is seen in the Fig. 24 at $\theta = 50°$. As time goes on, the exceeded energy is gradually separated ; one forming a first break with sharp spike and the other accumulating before the direct wave front, as seen in Figs. $25 \sim 27$ at $\theta = 60°$, $70°$, $80°$. Therefore, the large amplitude before the time $\tau_2' = 1$ is due to the disturbances generated at every point of the interface hit by the direct wave, and due to the higher velocity of propagation in this lower medium.

The transmitted wave in the lower medium is accompanied by the conical wave in the upper medium. And the energy of disturbance at and behind the conical wave front is supplied from the lower medium. Thus the large disturbance (marked by Ⓔ) of the transmitted wave before the direct wave front is again transmitted into the upper medium. This re-transmitted disturbance forms the phase of large amplitude (marked by Ⓑ) of the reflection before the time $\tau_1' = 1$.

(iii) Reflection ratio

The amplitude ratio of reflection to the direct wave at the time $\tau' = 1$ is obtained from (3.27) and (3.28) in spite of their infinite values, and is given by

$$R = \frac{dp_{10} + dp_{11}}{dp_0} \bigg|_{\tau'=1} = \frac{\sqrt{A} - \sqrt{B}}{A - B}$$

where A and B are given in (3.29). This ratio will show the variation of reflection coefficient with incident angle, the distance factor being cancelled out as a common factor. Results are illustrated in Fig. 28 for various velocity contrast.
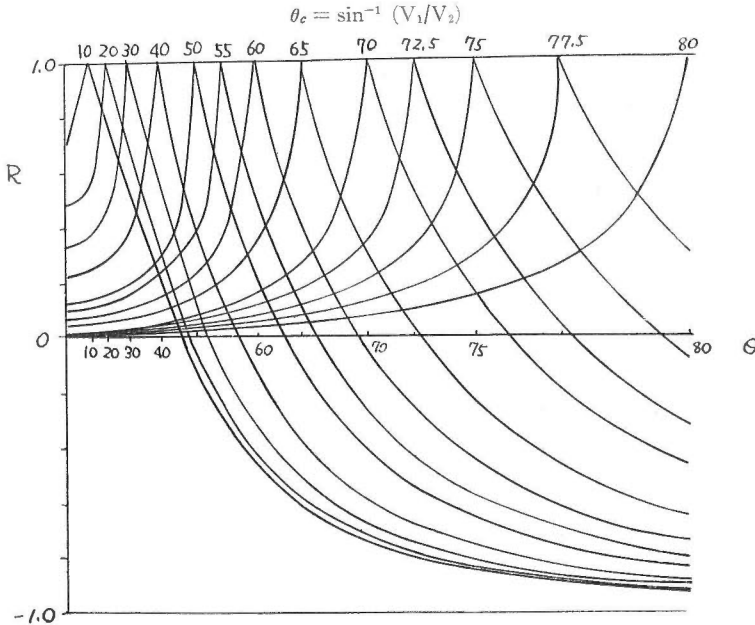

Fig. 28 Variation of reflection coefficient R with incident angle θ for various velocity contrast ; $\dfrac{V_1}{V_2} = \sin \theta_c$

The reflection coefficient increases with angle θ, and reaches unity at the critical angle. Then it decreases, and becomes negative value, meaning phase inversion, and approaches to minus unity as θ goes to $90°$. The point beyond which the phase inversion takes place is not exactly at the critical angle. It is located a little off the critical angle.

The increase of reflection coefficient with angle within the critical angle will be interpreted as a result of accumulation of disturbances which are generated at the interface by the direct wave and which propagate with the higher velocity in the lower medium. This picture is in agreement with mechanism described in the preceding paragraph (ii).

IV. Diffraction of an Acoustic Pressure Pulse by a Finite Fixed Plane in Liquid

IV. 1 Introduction

Diffracted wave from a fault has been partly used as an useful information in seismic prospecting. In these two or three years, lots of diffraction-like waves have been observed on the variable density presentation of the seismic continuous profile. It is the purpose of this chapter to obtain some characteristics for the nature of diffraction phenomena.

Since Sommerfeld gave the famous solution for diffraction of an acoustic wave by a plane screen, many investigators have studied this phenomena. Their works have been reviewed by Bouwkamp[2] and summarized in a book by Baker and Copson[1].*

In this chapter, the method of integral transformation is applied to diffraction of an acoustic pressure pulse with a cylindrical wave front by a finite fixed plane placed in liquid. Boundary conditions are formulated in IV. 2 and formal solutions are obtained in IV. 3. The inverse transformation of the formal solutions is evaluated by using convolution formula, which is different from the method used in the preceding chapters. Thus exact solutions of reflection and diffraction wave are obtained in IV. 4. Physical interpretations of diffraction phenomena are made in IV. 5, revealing many interesting features.

IV. 2 Boundary conditions

Let us consider the case where a finite fixed plane is placed in an infinite liquid medium, and a line source is located on the z-axis. Referring to the rectangular coordinate in Fig. 29, the fixed plane is placed in x-y plane at $-b < x < a$ and $z = 0$, and a line source is located at $z = f$, $x = 0$. For the convenience of calculation, the medium is devided into two regions by the plane at $z = 0$. The displacement potential, density and velocity are denoted by ϕ, ρ and V respectively. The suffixes 0, 1 and 2 refer to the source, region I and region II.

If we assume no energy transmission through the fixed plane from region I to region II, boundary conditions to be satisfied at $z = 0$ and $-\infty < x < \infty$ are expressed by

---

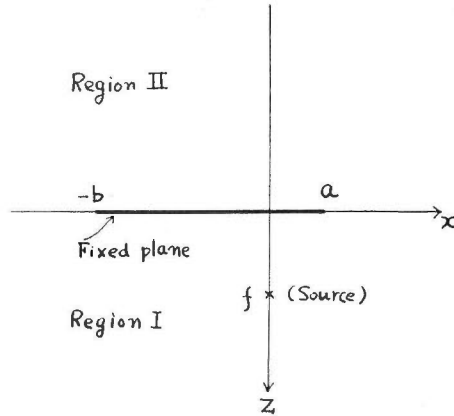* Recently deHoop[4] presented a elastodynamic diffraction theory.

Fig. 29

$$\rho \, \frac{\partial^2 \phi_1}{\partial t^2} = \rho \frac{\partial^2 \phi_2}{\partial t^2} + \rho \, \frac{\partial^2 g}{\partial t^2} \tag{4.1}$$

$$\frac{\partial \phi_1}{\partial z} = \frac{\partial \phi_2}{\partial z} \tag{4.2}$$

where

$$g\,(x,\,z,\,t) = 2\phi_0\,(x,\,o,\,t) \cdot u\,(a,\,-\,b\,;\,x) \tag{4.3}$$

$$u\,(a,\,-\,b\,;\,x) = \begin{cases} 0 \\ 1 \end{cases} \quad \text{for} \quad \begin{array}{l} x > a,\ x < -\,b \\ -\,b < x < a \end{array} \tag{4.4}$$

$$\phi_2\,(x,\,z,\,t) = \begin{cases} 0 \\ \phi_2\,(x,\,z,\,t) \end{cases} \quad \text{for} \quad \begin{array}{l} -\,b < x < a \ \textit{at}\ z = 0 \\ \text{other region} \end{array} \,. \tag{4.5}$$

These expressions of the boundary conditions, outside the fixed plane ($z = 0$, $x > a,\ x < -\,b$), become,

$$\begin{cases} \rho \, \dfrac{\partial^2 \phi_1}{\partial t^2} = \rho \, \dfrac{\partial^2 \phi_2}{\partial t^2} \\[2mm] \dfrac{\partial \phi_1}{\partial z} = \dfrac{\partial \phi_2}{\partial z} \end{cases} \tag{4.6}$$

and show continuity of stress and displacements. And, at the fixed plane, they become

$$\begin{cases} \rho \, \dfrac{\partial^2 \phi_1}{\partial t^2} = 2\rho \, \dfrac{\partial^2 \phi_0}{\partial t^2} \quad , \quad \phi_2 = 0 \\[2mm] \dfrac{\partial \phi_1}{\partial z} = \dfrac{\partial \phi_2}{\partial z} = 0 \end{cases} \tag{4.7}$$

and show the perfect reflection by a fixed plane, and no energy transmission through the plane.

Thus the problem of diffraction by a finite plane is reduced to a boundary value problem at an infinite interface. And the boundary value problem which

involves unit function in a finite region is solved by the method of integral transformation as is seen in the following sections.

IV. 3 Formal solutions

The Laplace-Fourier transformed wave equations are, as described in I. 4 of Chapter I,

$$\left\{ \frac{d^2}{dz^2} - (\xi^2 + h^2) \right\} \bar{\phi}_i (\xi, z, p) = 0 \qquad i = 1, 2 \qquad (4.8)$$

where $h^2 = p^2/V^2$. The Laplace-Fourier transform of the boundary conditions (4.1) (4.5) become

$$\left\{ \begin{array}{l} \bar{\phi}_1 (\xi, z, p) = \bar{\phi}_2 (\xi, z, p) + a_0 (p) \, \bar{g} (\xi) \\[2mm] \dfrac{\partial \bar{\phi}_1}{\partial z} = \dfrac{\partial \bar{\phi}_2}{\partial z} \end{array} \right. \qquad (4.9)$$

where

$$\begin{aligned} a_0 (p) \, \bar{g} (\xi) &= F \cdot L \left[g (x, z, t) \right]_{z=0} \\[2mm] &= \frac{1}{\sqrt{2\pi}} \int_{-\infty}^{\infty} \left\{ \int_0^{\infty} g (x, z, t) \, e^{-pt} \, dt \right\} e^{i\xi x} \, dx \bigg|_{z=0} \end{aligned} \qquad (4.10)$$

The general solutions of wave equations (4.8) in the transformed space are

$$\left\{ \begin{array}{l} \bar{\phi}_1 (\xi, z, p) = A (\xi, p) \, e^{-\sqrt{\xi^2+h^2}\, z} + \bar{\phi}_0 (\xi, z, p) \\[2mm] \bar{\phi}_2 (\xi, z, p) = B (\xi, p) \, e^{+\sqrt{\xi^2+h^2}\, z} \end{array} \right. \qquad (4.11)$$

and

$$\bar{\phi}_0 (\xi, z, p) = A_0 (\xi, p) \, e^{\mp \sqrt{\xi^2+h^2}\, (f-z)} \qquad \text{for} \quad z \lessgtr f \, . \qquad (4.12)$$

The coefficients A and B are determined by putting (4.11) (4.12) into (4.9);

$$\left\{ \begin{array}{l} A = \dfrac{1}{2} a_0 (p) \, \bar{g} (\xi) \\[4mm] B = A_0 \, e^{-\sqrt{\xi^2+h^2}\, f} - \dfrac{1}{2} a_0 (p) \, \bar{g} (\xi) \end{array} \right. \qquad (4.13)$$

Thus, the displacement potentials in the transformed space become

$$\left\{ \begin{array}{l} \bar{\phi}_1 (\xi, z, p) = A_0 \, e^{\mp \sqrt{\xi^2+h^2}\, (f-z)} + \dfrac{1}{2} a_0 (p) \, \bar{g} (\xi) \, e^{-\sqrt{\xi^2+h^2}\, z} \\[4mm] \bar{\phi}_2 (\xi, z, p) = A_0 \, e^{-\sqrt{\xi^2+h^2}\, (f-z)} - \dfrac{1}{2} a_0 (p) \, \bar{g} (\xi) \, e^{+\sqrt{\xi^2+h^2}\, z} \end{array} \right. \qquad (4.14)$$

Then the formal solutions of displacement potential in the original space are directly written down as

$$\phi_1 (x, z, t) = \phi_0 (x, z, t) + \phi_{refl} (x, z, t) \qquad (4.15)$$

$$\phi_2 (x, z, t) = \phi_0 (x, z, t) - L^{-1} \cdot F^{-1} \left\{ \frac{1}{2} a_0 (p) \, \bar{g} (\xi) \, e^{+\sqrt{\xi^2+h^2}\, z} \right\} \qquad (4.16)$$

42

where

$$\phi_{refl} \equiv L^{-1} \cdot F^{-1} \left\{ \frac{1}{2} \, a_0 \, (p) \; \bar{g} \, (\xi) \; e^{-\sqrt{\xi^2 + h^2} \; z} \right\} \tag{4.17}$$

$$\phi_0 = L^{-1} \cdot F^{-1} \left\{ A_0 \, (\xi, \, p) \; e^{-\sqrt{\xi^2 + h^2} \; (f-z)} \right\} \tag{4.18}$$

and L^{-1} and F^{-1} denote the operation of inverse Laplace transformation and inverse Fourier transformation respectively.

IV. 4 Evaluation of the inverse transformations

Evaluation of the inverse transformation is made by the following steps ; (1) give a form to the source function, (2) perform inverse Fourier transformation by using convolution formula, (3) change the order of integration, and (4) perform inverse Laplace transformation by using convolution formula.

Let us use the same source function that has been used in the preceding chapters ;

$$\phi_0 = \begin{cases} 0 & \\ \cosh^{-1} \, t/r/V & \end{cases} \quad \text{for} \quad \begin{array}{l} t < r/V \\ t > r/V \end{array} \tag{4.19}$$

$$r = \sqrt{x^2 + (f-z)^2}$$

and

$$A_0 \, (\xi, \, p) = \sqrt{\frac{\pi}{2}} \; \cdot \; \frac{1}{p} \; \cdot \; \frac{1}{\sqrt{\xi^2 + h^2}} \quad . \tag{4.20}$$

(i) Evaluation of $\phi_1 \, (x, \, z, \, t)$ in region I

In the region I, the term whose evaluation is required is ϕ_{refl} (4.17). Since the term ϕ_{refl} shows the inverse transformation of a product of $\frac{1}{2} \, a_0 \, (p) \, \bar{g} \, (\xi)$ and $e^{-\sqrt{\xi^2 + h^2} \; z}$, we use Fourier convolution formula* for the inversion. Thus we get for $z > 0$

$$\phi_{refl} = L^{-1} \cdot F^{-1} \left[\frac{1}{2} a_0 \, (p) \; \bar{g} \, (\xi) \times e^{-\sqrt{\xi^2 + h^2} \; z} \right]$$

$$= L^{-1} \left[\frac{1}{\sqrt{2\pi}} \int_{-\infty}^{\infty} u \, (a, \, -b ; \, \eta) \, \frac{1}{p} \, K_0 \left[h \sqrt{\eta^2 + f^2} \right] \frac{hz}{\sqrt{(x-\eta)^2 + z^2}} \right.$$

$$\left. K_1 \left[h \sqrt{(x-\eta)^2 + z^2} \right] d\eta \right]$$

$$= L^{-1} \left[\frac{1}{\sqrt{2\pi}} \int_{-b}^{a} \frac{1}{p} \, \frac{hz}{\sqrt{(x-\eta)^2 + z^2}} \, K_0 \left[h\sqrt{\eta^2 + f^2} \right] \cdot K_1 \left[h\sqrt{(x-\eta)^2 + z^2} \right] d\eta \right] \tag{4.21}$$

---

* Fourier convolution formula

$$F^{-1} \left[F \, (\xi) \; G \, (\xi) \right] = \frac{1}{\sqrt{2\pi}} \int_{-\infty}^{\infty} F \, (\xi) \; G \, (\xi) \; e^{-i\xi x} \; dx = \frac{1}{\sqrt{2\pi}} \int_{-\infty}^{\infty} g \, (\eta) \, f \, (x-\eta) \; d\eta$$

where $F \, (\xi)$ and $G \, (\xi)$ are the Fourier transforms of $f \, (x)$ and $g \, (x)$.

Next, we change the order of integration, namely we apply inverse Laplace transformation to the integrand of (4.21). Since the integrand of (4.21) has a form of product of K_0 and K_1, as functions of p, we use Laplace convolution formula*. Then we get

$$\phi_{refl} = \frac{1}{V\sqrt{2\pi}} \int_{-b}^{a} \frac{z}{V\sqrt{(x-\eta)^2 + z^2}}$$
$$\left[\int_0^t \frac{1}{\sqrt{(t-\tau)^2 - \frac{\eta^2 + f^2}{V^2}}} \cdot \frac{\tau}{\frac{\sqrt{(x-\eta)^2 + z^2}}{V} \cdot \sqrt{\tau^2 - \frac{(x-\eta)^2 + z^2}{V^2}}} \, d\tau \right] d\eta$$

(4.22)

If we denote $\sqrt{\eta^2 + f^2}/V_1 = t_1$ and $\sqrt{(x-\eta)^2 + z^2}/V = t_2$, the domain of integration in (4.22) is reduced to $t_2 < \tau < t - t_1$, because ϕ_{refl} vanishes for $\tau < t_2$ and $(t - \tau) < t_1$. Thus formula (4.22) becomes

$$\phi_{refl} = \frac{1}{V\sqrt{2\pi}} \int_{-b}^{a} \frac{z}{\{(x-\eta)^2 + z^2\}} \left[\int_{t_2}^{t-t_1} \frac{\tau \, d\tau}{\sqrt{(t-\tau)^2 - t_1^2}\sqrt{\tau^2 - t_2^2}} \right] d\eta \quad (4.23)$$

(ⅱ) Evaluation of $\phi_2(x, z, t)$ in region II

The representation of source function as a form of inverse transformation (4.18) leads it to another integral representation. Considering the integrand of (4.18) as a product of $\frac{1}{\sqrt{\xi^2 + h^2}} e^{-\sqrt{\xi^2 + h^2} f}$ and $e^{-\sqrt{\xi^2 + h^2} z}$, we use Fourier convolution formula, and we get

$$\phi_0 = L^{-1}\left[\frac{1}{V\sqrt{2\pi}} \int_{-\infty}^{\infty} \frac{1}{p} K_0 \left[h\sqrt{\eta^2 + f^2} \right] \frac{-hz}{\sqrt{(x-\eta)^2 + z^2}} K_1 \left[h\sqrt{(x-\eta)^2 + z^2} \right] d\eta \right]$$

(4.24)

Then ϕ_0 is combined with the second term of (4.16), forming a single term of integration with respect to η in the range $(-\infty < \eta < -b)$ and $(a < \eta < \infty)$. Then we again use Laplace convolution formula for the product of K_0 and K_1 in (4.24). Thus we get the final expression of the displacement potential in region II,

$$\phi_2(x, z, t) = \frac{1}{V\sqrt{2\pi}} \left(\int_{-\infty}^{-b} + \int_a^{\infty} \right) \left[\frac{-z}{\{(x-\eta)^2 + z^2\}} \int_{t_1}^{t-t_1} \frac{\tau}{\sqrt{(t-\tau)^2 - t_2^2}\sqrt{\tau^2 - t_1^2}} \, d\tau \right] d\eta.$$

(4.25)

Pressure solution is obtained from (4.23) and (4.25) by the relation

$$dp = -\rho \frac{\partial^2 \phi}{\partial t^2} \quad . \tag{4.26}$$

---

* Laplace convolution formula

$$L^{-1}[F(s) \, G(s)] = \int_0^t f(t-\tau) \, g(\tau) \, d\tau$$

where $F(s)$ and $G(s)$ are Laplace transforms of $f(t)$ and $g(t)$.

IV. 5 Interpretation

Following physical interpretations are derived from the solutions obtained in (4.23) and (4.25) for ; (i) wave front, (ii) mechanism of reflection, (iii) mechanism of diffraction in region I, (iv) amplitude variation with diffraction angle in region I, (v) mechanism of refraction (Huygens' principle), and (vi) mechanism of diffraction in region II.

For simplifying the explanation, the medium is devided into four regions ; referring to Fig. 30, reflection region, refraction region and diffraction region I and II.
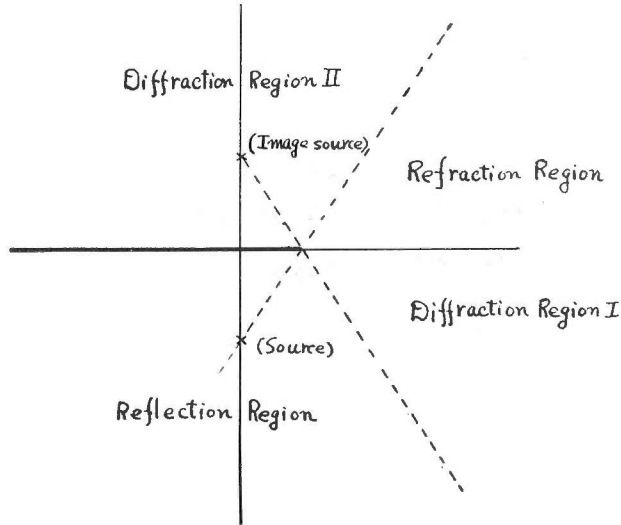

Fig.   30

(i)   Wave front

The first break wave front of ϕ_{refl} and ϕ_2 are determined by the smallest value of t in (4.23) and (4.25).   Because ϕ_{refl} and ϕ_2 have values in the range $t - t_1 > t_2$, the smallest value of t, from which time ϕ_{refl} and ϕ_2 begin to have values, is equal to $(t_1 + t_2)$. $(t_1 + t_2)$ is still the function of η.   Therefore, the arrival time of the first break, t_0, is expressed by

$$t_0 = \text{Smallest value of } (t_1 + t_2) \qquad\qquad (4.27)$$

where

$$\begin{cases} t_1 = \dfrac{1}{V} \sqrt{\eta^2 + f^2} \\[2mm] t_2 = \dfrac{1}{V} \sqrt{(x - \eta)^2 + z^2} \end{cases}$$

and the ranges of η are

$$\begin{cases} -b < \eta < a & \text{for} \quad \phi_{refl} \\ \quad \eta < -b,\ \eta > a & \text{for} \quad \phi_2 \end{cases} .$$

Let us examine the wave fronts due to a end point a, assuming b is very large. In the reflection region, t_0 becomes

$$t_0 = \text{Smallest value of } \frac{1}{V} (\rho_\eta^f + \rho)$$

where, referring to Fig. 31,

$$\begin{cases} \rho_\eta^f = V\sqrt{\eta^2 + f^2} \\ \rho_\eta = V\sqrt{(x-\eta)^2 + z^2} \\ -b < \eta < a \end{cases}.$$

Therefore the wave front of the first break of ϕ_{refl} in the reflection region is the circle with $z = -f$, $x = 0$, the image source point, as a center.

In the diffraction region I, t_0 becomes

$$t_0 = \frac{1}{V} [V\sqrt{a^2 + f^2} + V\sqrt{(x-a)^2 + z^2}]$$

because the range of η is $-b < \eta < a$. Therefore, the wave front of the first break of ϕ_{refl} in diffraction region I coincides with the circle with $x = a$, $z = 0$, the end point of the plane, as a center.

In the refraction region, referring to Fig. 32, t_0 becomes

$$t_0 = \text{Smallest value of } \frac{1}{V} (\rho_\eta^f + \rho_\eta)$$
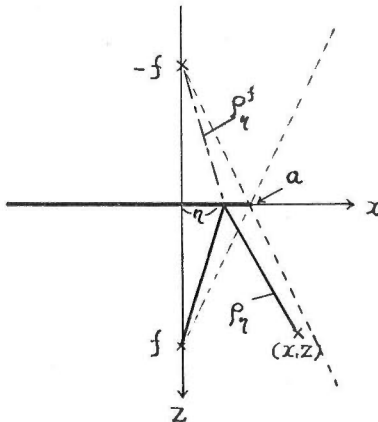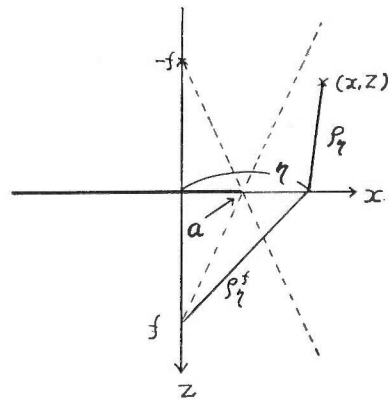

Fig. 31   Fig. 32

where the range of η is $\eta > a$ and $\eta < -b$. Therefore, the wave front of ϕ_2 in the refraction region is the circle with $z = f$, $x = 0$, the source point, as a center.

In the diffraction region II, t_0 becomes

$$t_0 = \frac{1}{V} [V\sqrt{a^2 + f^2} + V\sqrt{(x-a)^2 + z^2}]$$

because the range of η is $\eta > a$ and $\eta < -b$. The wave front is the circle

with $x = a$, $z = 0$, the end point of the plane, as a center.

All the wave fronts of the first break, thus obtained, are illustrated in Fig. 33. Perhaps a question will arise for the diffraction wave front in the reflection region and refraction region. The mathematical expression of the solution does not show this wave front. The question for the diffraction wave in these regions will be answered in following discussions.
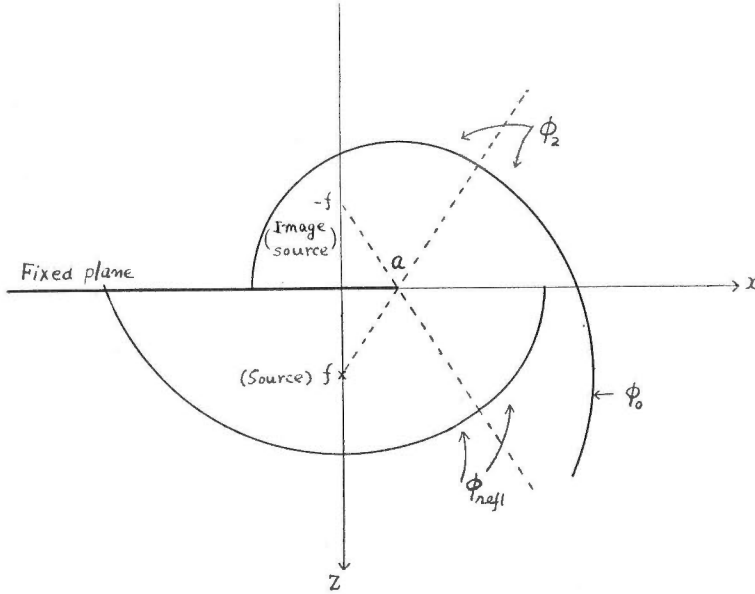

Fig. 33 Wave front of each term

(ii) Mechanism of reflection

Because an understanding of reflection mechanism is helpful for the interpretation of diffraction phenomena, let us examine reflection mechanism. Then, diffraction phenomena will be interpreted as a special case of reflection phenomena.

Reflection by an infinite fixed plane is obtained from equation (4.23), by putting $a = \infty$ and $- b = -\infty$;

$$\frac{1}{\sqrt{2\pi}} \int_{-\infty}^{\infty} \frac{z}{\{(x - \eta)^2 + z^2\}} \left[\int_{t_2}^{t-t_1} \frac{\tau d\tau}{\sqrt{(t-\tau)^2 - t_1^2}\sqrt{\tau - t_2^2}} \right] d\eta \qquad (4.28)$$

The second integration with respect to η shows that the wave form of the reflection wave at a certain point (x, z) in region I is made up of contributions from every point on the boundary. The first integration with respect to τ shows the time variation of each contribution. This will be interpreted as that every point on the boundary, when it is hit by a source wave, reflects back acoustic energy to all directions. And the reflected acoustic energy varies with time according to the source wave function. The transient reflection wave, which is observed at a certain point (x, z), is being formed with time by composing each contribution from every point on the boundary. The transient reflection wave form of an acoustic pulse will be completed when all the contributions have arrived at

the receiving point.

(iii) Mechanism of diffraction in region I

Comparing the formula of ϕ_{refl} (4.23) with the formula (4.28), it will be obvious that so-called diffraction phenomenon is nothing but a part of reflection phenomenon, reflection from a finite boundary. There will be no separated, particular wave which is so-called diffraction wave. This will be more naturally understood by looking at other features associated with diffraction.

(1) So-called diffraction wave, ϕ_{refl} in diffraction region I, is composed of reflections from boundary $-b < x < a$. And the path of each contribution is different from the path of geometrical optics (Snell's law).

(2) The end point of an reflection boundary is not the only factor which determines the characteristics of so-called diffraction wave. Other area of reflection boundary also contributes to the diffraction wave.

(3) The reflection wave in the reflection region is also affected by the finite boundary, and differs from the reflection wave from an infinite boundary.

(4) There is no additional acoustic energy besides reflection in the reflection region. So-called diffraction wave in reflection region will not exist, except an indication, if it were observed, of absence of energy contribution in the reflection wave form.

From the above features, so-called diffraction may be called "incomplete reflection", meaning that the diffraction is a part of reflection whose wave form is not completed due to the finite boundary of reflection.

(iv) Amplitude variation with diffraction angle in region I

A term in the integrand of (4.23), $z/\{(x - \eta)^2 + z^2\}$, gives a factor for an amplitude variation of diffraction wave. Because of

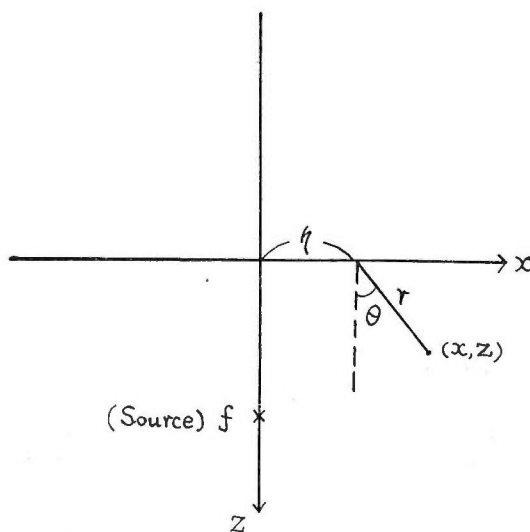$$\frac{z}{(x - \eta)^2 + z^2} = \frac{1}{r} \cos \theta$$

Fig. 34

referring to Fig. 34, the amplitude variation with diffraction angle will be mild. This factor also suggests that the contribution from a point of the boundary has the maximum at $\theta = 0$, on the vertical direction to the boundary, and vanishes at $\theta = \pi/2$, in the direction of the boundary.

(v) Mechanism of refraction ; Huygens' Principle

If we consider the case where the fixed plane vanishes, refraction wave in region II becomes

$$\frac{1}{\sqrt{2\pi}} \int_{-\infty}^{\infty} \frac{-zd\eta}{(x-\eta)^2 + z^2} \int_{t_2}^{t-t_1} \frac{\tau d\tau}{\sqrt{(t-\tau)^2 - t_1^2}\,\sqrt{\tau - t_2^2}} \qquad (4.29)$$

by putting $a = b = 0$ in equation (4.25). This shows that, if we assume a virtual boundary in liquid, transmitted wave is expressed by the composition of contributions from every point at the virtual boundary. This is nothing but Huygens' Principle. There is however, another information to be added to that principle. It is seen that that the newly born source at the boundary emits energy only to one half space*, to the direction of propagation, and that the energy has its maximum on the perpendicular direction to the boundary and decreases with direction by a factor $\cos\theta$ and vanishes at the direction $\theta = \pi/2$.

(vi) Mechanism of diffraction in region II

Comparing the formula of ϕ_2 (4.25) with (4.29), it will be obvious that so-called diffraction phenomenon in shadow region is nothing but a refraction phenomenon. Similar features as described in (iii) and (iv) in this section are seen for the mechanism of diffraction in shadow region. There will be no separated diffraction wave in the refraction region.

Summary and Conclusion

The propagation of transient elastic wave in 2-dimensions is investigated by the method of dual integral transformation. Laplace transformation is applied with respect to time coordinate, and Fourier transformation is applied with respect to one space coordinate. Both wave equations and boundary conditions are transformed, and formal solutions are obtained in the transformed space. Then inverse transformations of the formal solutions are evaluated by using the translation property and δ-function property of the Laplace transformation. By this method, mathematical expression for solving the problem are reduced to a simple form.

Chapter I. Exact solutions of transient elastic waves generated by surface forces are obtained at every point in an elastic solid. Spacial surface forces are treated as a consequence of Fourier transformation applied to one space coordinate.

Chapter II. The buried line source problem is re-written by the method of dual integral transformation developed in Chapter I. Exact solution of the transient elastic wave at every point in a medium is obtained. A comparison of the method of dual integral transformation and other methods are discussed in II. 4.

---

* It will be easily seen from (4.23) that ϕ_{refl} becomes zero in this case.

Chapter III. Reflection and refraction of an acoustic pressure pulse at a liquid-liquid interface is treated so as to clear up the basic picture of reflection and refraction phenomena. Exact solution of pressure form is obtained at every point in media and numerical examples are presented. Results obtained are as follows :

(1) The pressure form of the refracted wave has a sharp spike with considerable amplitude.

(2) The phase of reflected wave is inversed beyond the critical angle. However there is another phase of large amplitude just ahead of the reflected wave. Thus, reflection wave forms show the oscillatory feature.

(3) Even beyond the critical angle, there is a transmission of considerable energy from the direct wave into the lower medium.

(4) Reflection ratio of reflected wave to incident wave increases with incident angle. Beyond the critical angle it begins to decrease and becomes negative value meaning phase inversion. The point beyond which phase inversion takes place is located off the critical angle.

(5) From these results, an interpretation for the mechanism of reflection and refraction phenomena is described in detail in III. 4.

Chapter IV. Diffraction of an acoustic pressure pulse by a finite fixed plane is investigated. An application of the convolution formula to the inverse transformation leads the exact solution to a form of integral of elementary functions. Results obtained are as follows :

(1) Diffraction phenomenon is, in its nature, reflection and refraction phenomena, whose energy is supplied from a finite boundary.

(2) There will be no diffraction wave in the reflection and refraction regions (Fig. 30), except an indication, if it were observed, of absence of energy contribution in the reflected wave form.

(3) Reflected wave in the reflection region and refracted wave in the refraction region are also affected by the finite boundary.

(4) The amplitude variation of diffracted wave due to diffraction angle will be mild because of a factor $\cos \theta$ (cf. Fig. 34).

(5) Another mathematical expression is obtained which gives Hugyens' principle with the additional information. It is mathematically deduced that newly born source at the boundary emits energy only to one half space and the energy varies with direction by a factor $\cos \theta$.

The writer wishes to express his hearty thanks to Dr. K. Iida, Dr. H. Honda and Dr. Y. Sato, who gave him kind advices for the completion of this manuscript, and also to Dr. C. H. Dix, who kindly read the original manuscript of chapter IV.

References

1) Baker, B. B. & E. T. Copson : The mathematical theory of Huygens' principle, 2nd ed., Oxford Univ. Press, 1950

2) Bouwkamp, C. J. : Diffraction theory, Physical Society, Reports on Progress in Physics, Vol. 17, p. 35~100, 1954

3) Cagniard, L. : Réflexion et réfraction des ondes seismiques progressives, Gauthier-Villars & Cie., Paris, 1939

50

4) deHoop, A. T. : Representation theorems for the displacement in an elastic solid and their application to elastodynamic theory, 1958

5) Dix, C. H. : The method of Cagniard in seismic pulse problems, Geophys., Vol. 19, p. 722~738, 1954

6) Dix, C. H. : The mechanism of generation of long waves from explosions, Geophys., Vol. 20, p. 87~103, 1955

7) Dix, C. H. : The numerical computation of Cagniard's integral, Geophys., Vol. 23, p. 198~222, 1958

8) Garvin, W. W. : Exact transient solution of the buried line source problem, Proc. Roy. Acad. Soc., Ser. A, Vol. 234, p. 582~541, 1956

9) Hirono, T. : Mathematical theory on shallow earthquake, Geophys. Mag., Vol. 18, p. 1~116; Vol. 21, p. 1~97, 1948, 1949

10) Honda, H. & K. Nakamura : Notes on the problems on the motion of the surface of an elastic solid produced by a linear source, Science Rep. Tōhoku Univ., 5th Ser., Vol. 5, p. 58~66, 1953

11) Honda, H. & K. Nakamura : Notes on the reflection and refraction of SH-pulse emitted from a point source, Science Rep. Tōhoku Univ., 5th Ser., Vol. 5, p. 163~166, 1953

12) Honda, H. & K. Nakamura : On the reflection and refraction of the explosive sounds at the ocean bottom, Science Rep. Tōhoku Univ., 5th Ser., Vol. 4, p. 125~133, 1953

13) Honda, H. & K. Nakamura : On the reflection and refraction of the explosive sounds at the ocean bottom II, Science Rep. Tōhoku Univ., 5th Ser., Vol. 5, p. 70~84, 1954

14) Honda, H., K. Nakamura & A. Takagi : The Disturbance in a semi-infinite elastic solid due to a linear surface impulse, Science Rep. Tōhoku Univ., 5th Ser., Vol. 8, p. 86~92, 1956

15) Kasahara, K. : Experimental studies on the mechanism of generation of elastic waves 2, Bull. Earthq. Res. Inst., Vol. 31, p. 71, 1953

16) Kawasumi, H. : Reflection and refraction of a seismic wave, Zisin, Vol. 4, p. 277~307 (in Japanese), 1932

17) Lamb, H. : On the propagation of tremors over the surface of an elastic solid, Phil. Trans. Roy. Soc. London, Sect. A, Vol. 203, p. 1~42, 1904

18) Lapwood, E. R. : The disturbance due to a line source in a semi-infinite elastic medium, Phil. Trans. Roy. Soc. London, Sect. A, 841, Vol. 242, p. 63~100, 1949

19) Nakano, H. : On Rayleigy wave, Jap. Jour. Astor. and Geophys., Vol. 2, No. 5, p. 1~94, 1925

20) Sakai, T. : On the propagation of tremors over the plane surface of an elastic solid produced by an internal source, Geophys. Mag., Vol. 8, p. 1~71, 1934

21) Sneddon, I. N. : Fourier transforms, Mcgraw-Hill, 1951

22) Sneddon, I. N. : HANDBUCH DER PHYSIK, Band II, Mathematische Methoden II, Functional Analysis, Springer, 1955

23) Spencer, T. W. : Reflection of an acoustic pressure pulse from a liquid-solid plane boundary, Geophys., Vol. 21, p. 71~87, 1956

24) Sommerfeld, cf. Baker and Copson, 1950

25) Takeuchi, H. & N. Kobayashi : Propagation of tremors over the surface of an elastic solid, Jour. Phys. Earth, Vol. 2, p. 27~31, 1954

26) Takeuchi, H. & N. Kobayashi : Wave generations from line sources within ground, Jour. Phys. Earth, Vol. 3, p. 7~15, 1955

27) Takeuchi, H. & N. Kobayashi : Wave generation in a superficial layer resting on a semi-infinite lower layer, Jour. Phys. Earth, Vol. 4, p. 21~30, 1956

要　旨

弾性波パルスの伝播に関する研究

南　雲　昭三郎

　弾性波パルスの伝播に関する厳密解を求める方法は Cagniard[3] によつて開拓され，その難解な数学的表現は Dix[5] によつてラプラス変換の形式に書改められ，理解し易い，また，使い易い形式にまとめられた。その方法—Cagniard の方法を用いて，Dix[6]，Spencer[23]，Garvin[8] らは弾性波の発生伝播の問題を取扱い，半無限弾性体のレーリィ波の発生の機構や，液体—固体境界面における反射の機構などについて，従来より一層詳細な物理的像が得られてきた。

　この論文は，ラプラス変換がその1つであるところの，積分変換論をさらに二次元における弾性波伝播の理論に応用する方法を示したものである。すなわち，時間坐標についてラプラス変換を行なうのに加えて，一つの空間坐標についてフーリェ変換を行なう方法で，波動方程式，境界条件をラプラス・フーリェ変換し，変換された空間において形式的解を求め，逆変換によつて原空間における解を求めるものである。

　この方法によつて，数学的表現が簡単な形式にまとめられた。また Cagniard の方法において，解のフーリェ積分表示をラプラス変換積分の形に変数変換するテクニックが，ラプラス変換の移動則によつて論理的に自然に導入され，同時に δ-函数についてのラプラス変換公式によつて，積分路および変数変換について数学的物理的厳密さが与えられた。以上の方法によつて次のような問題を取扱つた。

　第1章において，半無限弾性体の表面に加えられた線状圧力，空間的拡がりをもつた圧力によつて生ずる弾性波パルスの問題を取扱つた。そこで積分変換を二重に応用する方法を詳しく説明し，弾性体内の任意の点における変位の厳密解を導いた。

　第2章においては，第1章で述べた方法によつて半無限弾性体内におかれた線状源から送り出された弾性波パルスの伝播の問題を取扱い，弾性体内の任意の点における変位の厳密解を導いた。この問題は Lapwood[18]，竹内，小林[26]，Garvin[8] らによつても取扱われているので，それらの方法の比較を行なつた (II. 4)。

　第3章においては，反射屈折現象の基本的物理像を明らかにするために，同様の方法によつて，液体—液体境界面における圧力波パルスの反射屈折の問題を取扱い，圧力波パルスの厳密解を求め，その数値計算を行なつた。その結果

　（1）　屈折波初動はかなりの振幅を有するスパイク状の波形をもつこと

　（2）　反射波の位相は臨界角以遠で反転するが，そのすぐ前に直接波と同位相の波があり，結局反射波として観測される波形は振動形をなすこと

　（3）　臨界角以遠でも，下方の速度の速い媒質へ，直接波からのエネルギーの伝達がかなりあること

　（4）　反射波パルスと直接波パルスの振幅比は，臨界角まで増大し，臨界角をすぎると減少し始め，次第に負の値になる(位相反転)こと，この位相反転を起こす入射角は臨界角ではなく，臨界角からかなり遠くであること

等のことが明らかになつた。以上のことから反射・屈折現象の物理的解釈を行なつた (III. 4)。

　第4章においては，液体中におかれた有限の固定平面による圧力波パルスの回折の問題を

取扱つた。積分変換の応用によつて，この問題が無限に拡がる境界面における境界値問題として厳密に取扱うことができた。逆変換の方法には，前3章のそれと異なり，畳み込み公式 (Convolution formula) を用いた。その結果厳密解が初等函数の積分の形に導かれた。その解について物理的解釈を行ない，その結果

（1）回折現象はその本質において反射屈折現象にほかならず，いわゆる回折波と呼ばれる波はスネルの法則を満足しない領域における反射波あるいは屈折波にほかならぬこと

（2）反射領域においては，反射波以外に回折波という特別な波は存在しないこと，たとえ存在するとしても反射波パルスにおけるエネルギーの欠損以外にはないこと

（3）反射領域における反射波，また屈折領域における屈折波の波形も，境界面が有限であることに影響され，無限に拡がつた境界面からのそれらと異なること

（4）回折波の振幅の，回折角度による減衰の仕方は $\cos \theta$（第34図参照）の項をもつているので，回折領域における急激な減衰は期待されないこと

（5）ホイゲンスの原理に対して，もう1つの数学的表現が与えられ，仮想された境界面における新しい波源は，入射波側にエネルギーを伝えないことが境界値問題の解として導かれ，また各波源から拡がつてゆく波は，境界面の法線方向に最大振幅をもち，角度とともに $\cos \theta$ の項によつて減少すること

などが明らかになつた。

The Geological Survey of Japan has published in the past several kinds of reports such as the Memoirs, the Bulletin, and the Report of the Geological Survey.

Hereafter, all reports will be published exclusively in the Reports of the Geological Survey of Japan. The Report will be consecutive to the numbers of the Report of the Imperial Geological Survey of Japan hitherto published. As a general rule, each issue of the Report will have one number, and for convenience's sake, the following classification according to the field of interest will be indicated on each Report.

A. Geology & allied sciences
- a. Geology
- b. Petrology and Mineralogy
- c. Paleontology
- d. Volcanology and Hot Spring
- e. Geophysics
- f. Geochemistry

B. Applied geology
- a. Ore deposits
- b. Coal
- c. Petroleum and Natural gas
- d. Underground water
- e. Agricultural geology
  Engineering geology
- f. Physical prospecting,
  Chemical prospecting & Boring

C. Miscellaneous

D. Annual Report of Progress

本所刊行の報文類の種目には従来地質要報・地質調査所報告等があつたが，今後はすべて刊行する報文は地質調査所報告に改めることとし，その番号は従来の地質調査所報告を追つて附けることにする．そして報告は1報文につき報告1冊を原則とし，その分類の便宜のために次の如くアルフアベットによる略号を附けることにする．

A　地質およびその基礎科学に関するもの
- a.　地　質
- b.　岩石・鉱物
- c.　古生物
- d.　火山・温泉
- e.　地球物理
- f.　地球化学

B　応用地質に関するもの
- a.　鉱　床
- b.　石　炭
- c.　石油・天然ガス
- d.　地下水
- e.　農林地質・土木地質
- f.　物理探鉱・化学探鉱および試錐

C　その他

D　事業報告